

Anomalous Thermal Hall Effects in Chiral Superconductors

Vudtiwat Ngampruetikorn* and J. A. Sauls†

Center for Applied Physics & Superconducting Technologies and
Department of Physics and Astronomy, Northwestern University, Evanston, IL 60208

(Dated: November 15, 2019)

We report theoretical results for the electronic contribution to thermal and electrical transport for chiral superconductors belonging to even or odd-parity E_1 and E_2 representations of the tetragonal and hexagonal point groups. Chiral superconductors exhibit novel transport properties that depend on the topology of the order parameter, topology of the Fermi surface, the spectrum of bulk Fermionic excitations, and – as we highlight – the structure of the impurity potential. The anomalous thermal Hall effect is shown to be sensitive to the structure of the electron-impurity t-matrix, as well as the winding number, ν , of the chiral order parameter, $\Delta(\mathbf{p}) = |\Delta(\mathbf{p})| e^{i\nu\phi_{\mathbf{p}}}$. For heat transport in a chiral superconductor with isotropic impurity scattering, i.e., point-like impurities, a transverse heat current is obtained for $\nu = \pm 1$, but vanishes for $|\nu| > 1$. This is not a universal result. For finite-size impurities with radii of order or greater than the Fermi wavelength, $R \geq \hbar/p_f$, the thermal Hall conductivity is finite for chiral order with $|\nu| \geq 2$, and determined by a specific Fermi-surface average of the differential cross-section for electron-impurity scattering. Our results also provide quantitative formulae for interpreting heat transport experiments for superconductors predicted to exhibit broken time-reversal and mirror symmetries.

I. INTRODUCTION

The search for an electronic analog of the chiral phase of superfluid ^3He has been pursued by many laboratories,^{1–3} driven in part by theoretical predictions of novel electronic properties of topological insulators and superconductors. Indeed chiral superfluids and superconductors are topological phases with gapless Fermionic excitations that reflect the momentum-space topology of the condensate of Cooper pairs. The A-phase of superfluid ^3He was definitively identified as a chiral p-wave superfluid by the observation of anomalous Hall transport of electrons moving through a quasiparticle fluid of chiral Fermions.^{4,5}

In 2D materials, chiral d-wave superconductivity is predicted for doped graphene^{6,7}, while a chiral p-wave state is proposed for MoS.⁸ For the 3D pnictide SrPtAs, where there is evidence from μSR of broken time-reversal symmetry onset at the superconducting transition,⁹ a chiral d-wave state has been proposed theoretically as the ground state.¹⁰ The perovskite superconductor, Sr_2RuO_4 , has been studied extensively and was proposed as a promising candidate for chiral p-wave superconductivity (E_u pairing with $\vec{\Delta} = \hat{\mathbf{d}}(p_x + ip_y)$), in part based on similarities of its normal-state Fermi-liquid properties with those of liquid ^3He .^{11,12} Observations of broken time-reversal symmetry from both μSR and Kerr rotation measurements support an identification of Sr_2RuO_4 as a chiral superconductor.^{13,14} However, experiments designed to detect the theoretically predicted chiral edge currents,¹⁵ or to test for the two-dimensionality of the E_u representation that is a necessary requirement to support a chiral ground state, so far are inconclusive, or report null results.^{16–19} Recent transport measurements also appear to conflict with the chiral p-wave identification based on the E_u representation; i.e. thermal conductivity measurements at low temperatures and as a function of magnetic field, which probe the low-energy quasiparticle excitation spectrum, are consistent with the nodal line structure of a d-wave order parameter, and inconsistent with the gap structure expected based on the E_u representation.^{20,21} The possibility that Sr_2RuO_4 is an even parity chiral superconductivity has so far not been ruled out.

The first superconductor reported to show experimental evidence of broken time-reversal symmetry was the heavy fermion superconductor, UPt_3 , based on μSR linewidth measurements.²² This experiment followed theoretical predictions of broken time-reversal symmetry in the B-phase of UPt_3 , i.e. the lower temperature superconducting phase.²³ Particularly striking is the relatively recent observation of the onset of Kerr rotation at the transition to the low-temperature B-phase of UPt_3 .²⁴ These results support the identification of a chiral superconducting phase of UPt_3 , and they also support the basic theoretical model of a multi-component order parameter belonging to a two-dimensional representation of the hexagonal point group, D_{6h} , in which a weak symmetry breaking field lifts the degeneracy of the two-component order stabilizing two distinct superconducting phases in zero magnetic field.^{23,25} In this theory the predicted A phase of UPt_3 is time-reversal symmetric with pronounced anisotropic pairing correlations in the hexagonal plane,^{26,27} is preferentially selected by the symmetry breaking field, and nucleates at $T_{c1} = 560\text{mK}$ as the first superconducting phase. The B-phase develops as the sub-dominant partner of the two-dimensional representation nucleates at $T_{c2} \approx 470\text{mK}$, such that the low-temperature superconducting phase spontaneously breaks both time-reversal and mirror-reflection symmetries, the latter defined by a plane containing the chiral axis which is aligned parallel (or anti-parallel) to the c-axis of UPt_3 .

There are four two-dimensional representations of D_{6h} : two even-parity representations, E_{1g} and E_{2g} , and two odd-parity representations, E_{1u} and E_{2u} , all of which allow for chiral ground states.^{28,29} The chiral ground states belonging to the E_1 and E_2 representations are defined by zeroes of the Cooper pair amplitude at points $\mathbf{p} = \pm p_f \hat{\mathbf{z}}$ on the Fermi surface that are protected by the topology of the orbital order parameter in momentum space, i.e. $\Delta(\mathbf{p}) = |\Delta(\mathbf{p})| e^{i\nu\phi_{\mathbf{p}}}$, where $\phi_{\mathbf{p}}$ is the azimuthal angle defining a point \mathbf{p} on the Fermi surface, and $\nu = \pm 1$ ($\nu = \pm 2$) for the E_1 (E_2) representations.³⁰ The bulk of the experimental evidence - thermodynamic, H-T phase diagram,^{28,31,32} thermal transport,^{33,34} ultra-sound,³⁵ Josephson tunneling,³ SANS³⁶ and optical spectroscopy measurements²⁴ - supports the identification of UPt_3 as an odd-parity supercon-

ductor with an order parameter belonging to the E_{2u} representation, *and* a chiral B-phase order parameter of the form, $\bar{\Delta}_{\pm}(\mathbf{p}) = \Delta_b(T) \hat{\mathbf{d}} \hat{p}_z (\hat{p}_x \pm i\hat{p}_y)^2 \sim \hat{\mathbf{d}} e^{\pm i2\phi_p}$. The vector $\hat{\mathbf{d}}$ is the quantization axis along which the spin-triplet Cooper pairs have zero spin projection, i.e. an equal-spin pairing (ESP) state.³¹ A key feature of the E_{2u} chiral order parameter is the winding number $\nu = \pm 2$. The Josephson interference experiment described in Ref. 3 can discriminate between $|\nu| = 1$ and $|\nu| = 2$ chiral ground states. Indeed the report of a π phase shift in the Fraunhofer pattern for the corner-SQUID geometry, combined with the observations of broken time-reversal symmetry,^{22,24} provides strong evidence in favor a $|\nu| = 2$ (E_{2u}) chiral B-phase of UPt₃. Nevertheless, the definitive proof of *bulk* chiral superconductivity awaits a zero-field bulk transport measurement that otherwise vanishes in the absence of broken time-reversal and mirror symmetries.

II. ANOMALOUS HALL TRANSPORT

The winding number of the order parameter for a chiral superconductor reflects the topology of the superconducting ground state. For a fully gapped chiral superconductor ν is related to the Chern number defined in terms of the Bogoliubov-Nambu Hamiltonian in 2D momentum space, or for chiral superconductors defined on a 3D Fermi surface the effective two-dimensional spectrum at fixed $p_z \neq 0$, $\mathcal{C}(p_z) = \frac{1}{2\pi} \int d^2p \Omega_z(\mathbf{p})$, where $\Omega_z(\mathbf{p})$ is the Berry curvature.³⁷ The result for the Chern number is $\mathcal{C}(p_z) = \nu$, which provides topological protection for a spectrum of chiral Fermions.

For 2D chiral phases there is a spectrum of massless chiral Fermions confined on the boundary (edge states) with the zero-energy state enforced by the bulk topology. However, for a chiral order parameter defined on a closed 3D Fermi surface there is also a bulk spectrum of gapless Weyl-Majorana Fermions with momenta near the nodal points $p_z = \pm p_f$, in addition to a *spectrum* of massless chiral Fermions confined on surfaces normal to the $[1,0,0]$ and $[0,1,0]$ planes.³⁸

A. Anomalous Edge Transport

In two dimensions for a fully gapped chiral p-wave ground state the spectrum of chiral edge Fermions is predicted to give rise to quantized heat and mass transport in chiral superfluids and superconductors.^{38–42} In particular, an anomalous thermal Hall conductance is predicted to be quantized, $K_{xy}/k_B T = \frac{\pi}{12} k_B/\hbar$ based on the low-energy effective field theory of the chiral edge states.^{39,43} This result is also obtained from the topology of the bulk order parameter combined with linear response theory based on the Bogoliubov Hamiltonian for 2D $p_x + ip_y$ topological superconductors.⁴²

For a chiral superconductor defined on a 3D Fermi surface an anomalous thermal Hall current is predicted, but is not quantized in units of a fundamental quantum of conductance. Based on the linear response theory of Qin et al.,⁴³ Goswami and Nevidomsky obtained a result for the anomalous thermal Hall conductivity of the B-phase of UPt₃ for $T \ll T_{c2}$,³⁷

$$\kappa_{xy}/k_B T = \nu \frac{\pi}{6} \frac{k_B}{\hbar} \left(\frac{\Delta p}{2\pi\hbar} \right). \quad (1)$$

The anomalous thermal Hall conductivity reflects the number of branches of chiral Fermions confined on the $[1,0,0]$ or $[0,1,0]$ surface, i.e. $|\nu| = 2$ for the E_{2u} chiral ground state. The non-universality of the thermal Hall conductivity is reflected by the term Δp , which is the “distance” between the two topologically protected $\nu = 2$ Weyl points at $\hat{p}_z = \pm 1$ on a projected surface containing the chiral axis; e.g. $\Delta p = 2p_f$ for a spherical Fermi surface.³⁷

Thus, heat transport experiments could decisively identify the broken symmetries and topology of superconductors predicted to exhibit chiral order. The thermal conductivity depends on both the topology of the order parameter and the Fermi surface. The anomalous thermal Hall effect, in which a temperature gradient generates heat currents perpendicular to it, results from broken time-reversal and mirror symmetries – a direct signature of chiral pairing.⁴⁴ A zero-field thermal Hall experiment can also be used as signature of chiral edge states. However, zero-field Hall transport has remained elusive thus far.

B. Impurity-Induced Anomalous Transport

Here we consider zero-field Hall transport resulting from electron-impurity interactions in the bulk of the superconductor, which we show are easily several orders of magnitude larger than the edge contribution. There are theoretical predictions for the impurity-induced anomalous thermal Hall effect in chiral superconductors, based on point-like impurities.^{45–47} As we show, the point-like impurity model, which includes only s-wave quasiparticle-impurity scattering, predicts zero Hall response except for Chern number $\nu = \pm 1$, i.e. only for chiral p-wave superconductors.⁴⁵

In the following we present a self-consistent theory incorporating the effects of finite-size impurities and show that such effects cannot be ignored in a quantitative description of Hall transport in chiral superconductors. Experimental observation of an impurity-induced anomalous thermal Hall effect would provide a definitive signature of chiral superconductivity. The bulk effect can easily dominate the edge state contribution to the anomalous Hall current, except in ultra-pure fully gapped chiral superconductors.

III. TRANSPORT THEORY

We start from the Keldysh extension⁴⁸ of the transport-like equations originally developed by Eilenberger, Larkin and Ovchinnikov for equilibrium states of superconductors,^{49,50} and extended by Larkin and Ovchinnikov to describe superconductors out of equilibrium.⁵¹ This formalism is referred to as “quasiclassical theory”. For reviews see Refs. 52–54. The quasiclassical theory is formulated in terms of 4×4 matrix propagators for Fermionic quasiparticles and Cooper pairs that describe the space-time evolution of their non-equilibrium distribution functions, as well as the dynamical response of the low-energy spectral functions and the superconducting order parameter. Here we are interested in the response to static, or low-frequency, thermal gradients and external forces that couple to energy, mass and charge currents. We follow as much as possible the notation and conventions of theory developed for thermal transport in unconventional superconductors by Graf et al.⁵⁵

A. Keldysh-Eilenberger Equations

The quasiclassical transport equations are matrix equations in particle-hole (Nambu) space which describe the dynamics of quasiparticle excitations and Cooper pairs. Physical properties, such as the spectral density, currents or response functions are expressed in terms of components of the Keldysh matrix propagator,

$$\check{G}(\mathbf{p}, \varepsilon; \mathbf{r}, t) = \begin{pmatrix} \hat{g}^R & \hat{g}^K \\ 0 & \hat{g}^A \end{pmatrix}, \quad (2)$$

where $\hat{g}^{R,A,K}(\mathbf{p}, \varepsilon; \mathbf{r}, t)$ are the 4×4 retarded (R), advanced (A) and Keldysh (K) matrix propagators.

The nonequilibrium dynamics is described by a transport equation for the Keldysh (K) propagator,

$$\begin{aligned} & \hat{H}^R \circ \hat{g}^K(\mathbf{p}, \mathbf{r}; \varepsilon, t) - \hat{g}^K \circ \hat{H}^A(\mathbf{p}, \mathbf{r}; \varepsilon, t) \\ & + \hat{g}^R \circ \hat{\Sigma}^K(\mathbf{p}, \mathbf{r}; \varepsilon, t) - \hat{\Sigma}^K \circ \hat{g}^A(\mathbf{p}, \mathbf{r}; \varepsilon, t) \\ & + i\mathbf{v}_\mathbf{p} \cdot \nabla \hat{g}^K(\mathbf{p}, \mathbf{r}; \varepsilon, t) = 0, \end{aligned} \quad (3)$$

as well as transport equations for the retarded and advanced propagators,

$$\left[\hat{H}^{R,A}, \hat{g}^{R,A} \right]_\circ + i\mathbf{v}_\mathbf{p} \cdot \nabla \hat{g}^{R,A}(\mathbf{p}, \mathbf{r}; \varepsilon, t) = 0, \quad (4)$$

where

$$\hat{H}^{R,A}(\mathbf{p}, \mathbf{r}; \varepsilon, t) = \varepsilon \hat{\tau}_3 - \hat{v}(\mathbf{p}, \mathbf{r}; t) - \hat{\Sigma}^{R,A}(\mathbf{p}, \mathbf{r}; \varepsilon, t), \quad (5)$$

is defined in terms of the excitation energy, ε , the coupling to external fields, \hat{v} , and the self-energies, $\hat{\Sigma}^{R,A}$. Pairing correlations, as well as effects of scattering by impurities, phonons and quasiparticles are described by the self-energies, $\hat{\Sigma}^{R,A,K}$. The convolution product (\circ -product) appearing in Eqs. (3-4), in the mixed energy-time representation, is defined by,

$$\hat{A} \circ \hat{B}(\varepsilon; t) = e^{\frac{i}{2}[\partial_\varepsilon^A \partial_t^B - \partial_t^A \partial_\varepsilon^B]} \hat{A}(\varepsilon; t) \hat{B}(\varepsilon; t). \quad (6)$$

Note that ε is the excitation energy and t is the external time variable. The operator expansion for the convolution

$$\hat{g}^{R,A,K} = \begin{pmatrix} g^{R,A,K} + \mathbf{g}^{R,A,K} \cdot \boldsymbol{\sigma} & (f^{R,A,K} + \mathbf{f}^{R,A,K} \cdot \boldsymbol{\sigma}) i\sigma_y \\ i\sigma_y (\bar{f}^{R,A,K} + \bar{\mathbf{f}}^{R,A,K} \cdot \boldsymbol{\sigma}) & \bar{g}^{R,A,K} - \bar{\mathbf{g}}^{R,A,K} \cdot \boldsymbol{\sigma}_y \sigma_y \end{pmatrix}. \quad (10)$$

The 16 matrix elements of $\hat{g}^{R,A,K}$ are expressed in terms of 4 spin-scalars ($g^{R,A,K}, \bar{g}^{R,A,K}, f^{R,A,K}, \bar{f}^{R,A,K}$) and 4 spin-vectors ($\mathbf{g}^{R,A,K}, \bar{\mathbf{g}}^{R,A,K}, \mathbf{f}^{R,A,K}, \bar{\mathbf{f}}^{R,A,K}$). All matrix elements are functions of \mathbf{p} , ε , \mathbf{r} and t . The spin scalars $g^{R,A,K}, \bar{g}^{R,A,K}$ determine spin-independent properties such as the charge, mass and heat current densities, $\mathbf{j}_e(\mathbf{r}, t)$, $\mathbf{j}_m(\mathbf{r}, t)$ and $\mathbf{j}_q(\mathbf{r}, t)$, as well as the local density of states

$$N(\varepsilon; \mathbf{r}, t) = N_f \int d\mathbf{p} \left[-\frac{1}{\pi} \text{Im} \frac{1}{2} \text{Tr} \left\{ \hat{\tau}_3 \hat{g}^R(\mathbf{p}, \varepsilon; \mathbf{r}, t) \right\} \right], \quad (11)$$

product is particularly useful if the external timescale, $t \sim \omega^{-1}$ is slow compared to the typical internal dynamical timescales, \hbar/Δ and τ , i.e. $\omega \ll |\varepsilon| \sim \Delta$ and $\omega \ll 1/\tau$. In this limit we can expand Eq. (6),⁵⁶

$$\hat{A} \circ \hat{B}(\varepsilon; t) \approx \hat{A}(\varepsilon; t) \hat{B}(\varepsilon; t) + \frac{i}{2} \left[\frac{\partial \hat{A}}{\partial \varepsilon} \frac{\partial \hat{B}}{\partial t} - \frac{\partial \hat{A}}{\partial t} \frac{\partial \hat{B}}{\partial \varepsilon} \right]. \quad (7)$$

The quasiclassical transport equations are supplemented by the normalization conditions,^{49,50}

$$\hat{g}^{R,A} \circ \hat{g}^{R,A} = -\pi^2 \hat{1}, \quad (8)$$

$$\hat{g}^R \circ \hat{g}^K - \hat{g}^K \circ \hat{g}^A = 0, \quad (9)$$

B. Quasiclassical Propagators

The quasiclassical propagators are 4×4 -matrices whose structure describes the internal quantum-mechanical degrees of freedom of quasi-particles and quasi-holes. In addition to spin, the particle-hole degree of freedom is of fundamental importance to our understanding of superconductivity. In the normal state of a metal or Fermi liquid there is no quantum-mechanical coherence between particle and hole excitations. By contrast, the distinguishing feature of the superconducting state is the existence of quantum mechanical coherence between normal-state particle and hole excitations. Particle-hole coherence is the origin of persistent currents, Josephson effects, Andreev scattering, flux quantization, and all other nonclassical superconducting effects. The quasiclassical propagators are directly related to density matrices which describe the quantum-statistical state of the internal degrees of freedom. Nonvanishing off-diagonal elements in the particle-hole density matrix are indicative of superconductivity, indeed the onset of non-vanishing off-diagonal elements is the signature of the superconducting transition.

The Nambu matrix structure of the propagators and self energies is

where N_f is the normal-state density of states at the Fermi energy. The integration is over the Fermi surface *weighted* by the angle-resolved normal density of states at the Fermi surface, $n(\mathbf{p})$, normalized to

$$\int d\mathbf{p} (\dots) \equiv \int dS_{\mathbf{p}} n(\mathbf{p}) (\dots) \text{ with } \int dS_{\mathbf{p}} n(\mathbf{p}) = 1. \quad (12)$$

The current densities are determined Fermi-surface averages over the elementary currents, $[e\mathbf{v}_\mathbf{p}]$, mass, $[m\mathbf{v}_\mathbf{p}]$, and energy, $[\varepsilon\mathbf{v}_\mathbf{p}]$, weighted by the scalar components of

the diagonal Keldysh propagator. In particular, the charge and heat current densities are given by

$$\mathbf{j}_e(\mathbf{r}, t) = N_f \int d\mathbf{p} \int \frac{d\varepsilon}{4\pi i} [e\mathbf{v}_\mathbf{p}] \text{Tr} \{ \widehat{\tau}_3 \widehat{g}^K(\mathbf{p}, \varepsilon; \mathbf{r}, t) \}, \quad (13)$$

$$\mathbf{j}_q(\mathbf{r}, t) = N_f \int d\mathbf{p} \int \frac{d\varepsilon}{4\pi i} [\varepsilon \mathbf{v}_\mathbf{p}] \text{Tr} \{ \widehat{g}^K(\mathbf{p}, \varepsilon; \mathbf{r}, t) \}. \quad (14)$$

The off-diagonal components, $f^{R,A,K}$ and $\mathbf{f}^{R,A,K}$, are the anomalous propagators that characterize the pairing correlations of the superconducting state. Spin-singlet pairing correlations are encoded in f^K , while \mathbf{f}^K is the measure of spin-triplet pairing correlations. Pair correlations develop spontaneously at temperatures below the superconducting transition temperature T_c . The anomalous propagators are not directly measurable, but the correlations they measure are observable via their coupling to the ‘‘diagonal’’ propagators, $g^{R,A,K}$ and $\mathbf{g}^{R,A,K}$, through the transport equations.

C. Coupling to External and Internal Forces

The couplings of low-energy excitations to electromagnetic fields are defined in terms of the scalar and vector potentials,

$$\widehat{v}_{\text{EM}} = e \varphi(\mathbf{r}, t) \widehat{\tau}_3 + \frac{e}{c} \mathbf{v}_\mathbf{p} \cdot \mathbf{A}(\mathbf{r}, t) \widehat{\tau}_3. \quad (15)$$

Note that $e\widehat{\tau}_3$ encodes the charge coupling of both particle and hole excitations to the electromagnetic field. The magnetic field also couples to the quasiparticles and pairs via the Zeeman energy, $\widehat{v}_z = \gamma \widehat{\mathbf{S}} \cdot \mathbf{B}(\mathbf{r}, t)$, where $\mathbf{B} = \nabla \times \mathbf{A}$, γ is the gyromagnetic ratio of the normal-state quasiparticles, and $\widehat{\mathbf{S}} = \frac{1}{2}(\widehat{1} + \widehat{\tau}_3)\sigma - \frac{1}{2}(\widehat{1} - \widehat{\tau}_3)\sigma_y \sigma_y$ is the Nambu representation of the Fermion spin operator.

Mean-Field Self-Energies

Superconductors driven out of equilibrium are also subject to internal forces on quasiparticles and Cooper pairs, originating from electron-electron, electron-phonon and electron-impurity interactions. These interactions enter the quasiclassical theory as self-energy terms, $\widehat{\Sigma}^{R,A,K}$, in the transport Eqs. 3, 4, and 5. We include self-energies that contribute to leading order in expansion parameters, $s = \{1/k_f \xi, k_B T_c / E_f, 1/k_f \ell, \hbar / \tau E_f \Delta / E_f \dots\} \ll 1$ that define the low-energy, long-wavelength region of validity of Landau Fermi-liquid theory, and its extension to include BCS condensation.^{52,54,57}

The leading order contributions to the self-energy from quasiparticle-quasiparticle interactions correspond the mean-field self-energies, $\widehat{\Sigma}_{\text{mf}}^{R,A,K}$, in the particle-hole (Landau) and particle-particle (Cooper) channels, and are represented by Eqs. 16 and 17, respectively,

$$\widehat{\Sigma}(\mathbf{p}) = \int d\mathbf{p}' \int \frac{d\varepsilon'}{4\pi i} [A^s(\mathbf{p}, \mathbf{p}') g^K(\mathbf{p}', \varepsilon') \widehat{1} + A^a(\mathbf{p}, \mathbf{p}') \mathbf{g}^K(\mathbf{p}', \varepsilon') \cdot \boldsymbol{\sigma}], \quad (16)$$

$$\widehat{\Delta}(\mathbf{p}) = - \int d\mathbf{p}' \int \frac{d\varepsilon'}{4\pi i} [\mu^s(\mathbf{p}, \mathbf{p}') f^K(\mathbf{p}', \varepsilon') i\sigma_y + \mu^t(\mathbf{p}, \mathbf{p}') \mathbf{f}^K(\mathbf{p}', \varepsilon') \cdot i\boldsymbol{\sigma}\sigma_y]. \quad (17)$$

Note that $\widehat{\Sigma}$ and $\widehat{\Delta}$ represent the upper row of the Nambu matrix, $\widehat{\Sigma}_{\text{mf}}$. Since the mean-field self-energies are independent of ε , $\widehat{\Sigma}_{\text{mf}}^R = \widehat{\Sigma}_{\text{mf}}^A = \widehat{\Sigma}_{\text{mf}}$, and $\widehat{\Sigma}_{\text{mf}}^K = 0$. The vertex, $A(\mathbf{p}, \mathbf{p}')$, in Eq. 16 represents the quasiparticle interactions in the particle-hole channel. In the non-relativistic limit these interactions are spin-rotation invariant, in which case there are two real amplitudes: the spin-independent quasiparticle-quasiparticle interaction, $A^s(\mathbf{p}, \mathbf{p}')$, the *exchange* term, $A^a(\mathbf{p}, \mathbf{p}')$, describing the spin-dependent quasiparticle-quasiparticle interaction. These interactions are defined by the renormalized four-point vertex in the forward-scattering limit for quasiparticles with momenta and energies confined to the Fermi surface, i.e. $|\mathbf{p}| = |\mathbf{p}'| = p_f$ and $\varepsilon = \varepsilon' = 0$, which is a good approximation in the Fermi-liquid regime far from a quantum critical point. Thus, the propagator is integrated over the low-energy bandwidth defined by $f(\dots) \equiv \int_{-\varepsilon_c}^{+\varepsilon_c} (\dots)$, and the corresponding self-energies depend on the direction of the quasiparticle momentum on the Fermi surface, but are independent of ε .

In the Cooper channel the mean-field self energy from quasiparticle interactions is given by Eq. 17. The vertex labeled by μ^* separates in terms of an even-parity, spin-singlet interaction, $\mu^s(\mathbf{p}, \mathbf{p}')$, and an odd-parity, spin-triplet interaction, $\mu^t(\mathbf{p}, \mathbf{p}')$, the latter resulting from exchange symmetry in the non-relativistic limit.⁵⁸ In a rota-

tionally invariant Fermi liquid like liquid ³He, the interactions in the Cooper channel further separate according to the irreducible representations of the rotation group in three dimensions, $\text{SO}(3)_L$,

$$\mu^{s(t)}(\mathbf{p}, \mathbf{p}') = \sum_l^{\text{even (odd)}} \mu_l \sum_{m=-l}^{+l} \mathcal{Y}_{l,m}^*(\hat{\mathbf{p}}) \mathcal{Y}_{l,m}(\hat{\mathbf{p}}'), \quad (18)$$

which are labeled by the orbital angular momentum quantum number $l \in \{0, 1, 2, \dots\}$, with the basis functions given by the spherical harmonics $\{\mathcal{Y}_{l,m}(\hat{\mathbf{p}})\}$, normalized to $\int d\mathbf{p} \mathcal{Y}_{l,m}(\hat{\mathbf{p}}) \mathcal{Y}_{l',m'}(\hat{\mathbf{p}}') = \delta_{ll'} \delta_{mm'}$. The Cooper instability occurs in the pairing channel defined by the most attractive interaction, μ_l , which for ³He is the odd-parity, spin-triplet ($S = 1$), $l = 1$ (p-wave) channel.

For strongly correlated materials Cooper pairing is mediated by quasiparticle-quasiparticle interactions. This is necessarily the case in a single-component Fermi system like liquid ³He, and is prevalent in strongly correlated electronic compounds such as the heavy-fermion superconductors, UPt₃ and URu₂Si₂, and unconventional superconductors like Sr₂RuO₄, all of which exhibit experimental signatures of broken time-reversal symmetry by the superconducting state. For these superconductors the pairing channel belongs to an irreducible representation of the crystal point group. Equation 18 holds with l summed over

the irreducible representations of the point group, the second sum m is over the set of orthogonal basis functions, $\{\mathcal{Y}_{lm}(\mathbf{p})|m \in \text{irrep}_l\}$, that span the irrep labeled by l . For materials with hexagonal point symmetry, e.g. UPT_3 , we consider the four two-dimensional ‘‘E-reps’’: even parity E_{1g} and E_{2g} representations and odd-parity E_{1u} and E_{2u} . All four E-reps allow for a chiral ground state with minimum Chern numbers of $\nu = \pm 1$ ($E_{1g(u)}$) or $\nu = \pm 2$ ($E_{2g(u)}$).

Impurity Self-Energy

The effects of impurity disorder originate from the quasiparticle-impurity vertex, $\check{u}(\mathbf{p}, \mathbf{p}')$, represented by the dotted-line vertex in Eq. 19, which corresponds to the transition matrix element for elastic scattering of a quasiparticle with momentum \mathbf{p} to the point \mathbf{p}' on the Fermi surface. Multiple scattering of quasiparticles and quasiholes by an impurity is described by the Bethe-Salpeter equation shown in Eq. 19.

$$\check{t}(\mathbf{p}', \mathbf{p}; \varepsilon) = \check{u}(\mathbf{p}', \mathbf{p})$$

$$+ N_f \int d\mathbf{p}'' \check{u}(\mathbf{p}', \mathbf{p}'') \check{g}(\mathbf{p}'', \varepsilon) \check{t}(\mathbf{p}'', \mathbf{p}; \varepsilon), \quad (19)$$

where $\check{t}(\mathbf{p}', \mathbf{p}; \varepsilon)$ is the t-matrix for quasiparticle-impurity scattering, and $\check{g}(\mathbf{p}; \varepsilon)$ is the quasiclassical Keldysh matrix propagator for particles, holes and Cooper pairs.

The leading-order contribution to the configurational-averaged self energy is then determined by scattering of quasiparticles off an uncorrelated, random distribution of statistically equivalent impurities with average density, n_{imp} ,

$$\check{\Sigma}_{\text{imp}}(\mathbf{p}; \varepsilon) = n_{\text{imp}} \check{t}(\mathbf{p}, \mathbf{p}; \varepsilon) = \begin{pmatrix} \hat{\Sigma}_{\text{imp}}^R & \hat{\Sigma}_{\text{imp}}^K \\ 0 & \hat{\Sigma}_{\text{imp}}^A \end{pmatrix} \quad (20)$$

where $\check{t}(\mathbf{p}, \mathbf{p}; \varepsilon)$ is the t-matrix evaluated self-consistently in the forward-scattering limit. Thus, the Nambu-matrix components of the impurity Keldysh self energy, $\hat{\Sigma}_{\text{imp}}^{R,A,K}(\mathbf{p}, \mathbf{r}; \varepsilon, t) = n_{\text{imp}} \hat{t}^{R,A,K}(\mathbf{p}, \mathbf{p}, \mathbf{r}; \varepsilon, t)$, are determined by the corresponding components of the t-matrix,

$$\hat{t}^{R,A}(\mathbf{p}', \mathbf{p}, \mathbf{r}; \varepsilon, t) = u(\mathbf{p}', \mathbf{p}) + N_f \int d\mathbf{p}'' u(\mathbf{p}', \mathbf{p}'') \hat{g}^{R,A}(\mathbf{p}'', \mathbf{r}; \varepsilon, t) \circ \hat{t}^{R,A}(\mathbf{p}'', \mathbf{p}, \mathbf{r}; \varepsilon, t) \quad (21)$$

$$\hat{t}^K(\mathbf{p}', \mathbf{p}, \mathbf{r}; \varepsilon, t) = N_f \int d\mathbf{p}'' \hat{t}^R(\mathbf{p}', \mathbf{p}'', \mathbf{r}; \varepsilon, t) \circ \hat{g}^K(\mathbf{p}'', \mathbf{r}; \varepsilon, t) \circ \hat{t}^A(\mathbf{p}'', \mathbf{p}, \mathbf{r}; \varepsilon, t). \quad (22)$$

Before proceeding to non-equilibrium quasiparticle transport we need to discuss the equilibrium state, including the effects of impurity scattering, on the equilibrium-states of chiral superconductors and superfluids.

IV. EQUILIBRIUM

For homogeneous systems in equilibrium the transport equations for the retarded and advanced propagators reduce to

$$[\varepsilon \hat{\tau}_3 - \hat{\Delta}(\mathbf{p}) - \hat{\Sigma}_{\text{imp}}^{R,A}(\mathbf{p}; \varepsilon), \hat{g}^{R,A}(\mathbf{p}; \varepsilon)] = 0, \quad (23)$$

where $\hat{\Delta}(\mathbf{p})$ is the mean-field order parameter and $\hat{\Sigma}_{\text{imp}}(\mathbf{p}; \varepsilon)$ is the equilibrium self-energy due to quasiparticle-impurity scattering. We consider the low-temperature limit in which the thermal populations of quasiparticles and phonons are sufficiently small that we can neglect quasiparticle-quasiparticle scattering and quasiparticle-phonon scattering contributions to the self energy. Thus, we retain only the mean-field pairing self energy and impurity self energy resulting from elastic quasiparticle-impurity scattering. The propagator is also constrained by the normalization condition, which for equilibrium reduces to matrix multiplication,

$$[\hat{g}^{R,A}(\mathbf{p}, \varepsilon)]^2 = -\pi^2 \hat{1}. \quad (24)$$

A chiral superconducting ground state is defined by spontaneous breaking of time-reversal and mirror symmetries by the orbital state of the Cooper pairs. Thus, we restrict our analysis to *unitary* superconductors in which the

4×4 Nambu matrix order parameter obeys the condition,

$$\hat{\Delta}(\mathbf{p})^2 = -|\Delta(\mathbf{p})|^2 \hat{1}. \quad (25)$$

Unitary states preserve time-reversal symmetry with respect to the spin-correlations of the pairing state. In the clean limit $|\Delta(\mathbf{p})|$ is the energy gap for quasiparticles with momentum \mathbf{p} near the Fermi surface, i.e. the Bogoliubov quasiparticle excitation energy is doubly degenerate with respect to spin and given by $E_{\mathbf{p}} = \sqrt{\xi_{\mathbf{p}}^2 + |\Delta(\mathbf{p})|^2}$, with $\xi_{\mathbf{p}} = v_f(|\mathbf{p}| - p_f)$ and $\Delta(\mathbf{p})$ defined for \mathbf{p} on the Fermi surface. The unitarity condition is necessarily satisfied by spin-singlet pairing states, and is also the case for all known spin-triplet superconductors in which the parent state in zero external field is non-magnetic.⁵⁹ An important class of unitary triplet states are the equal-spin-pairing (ESP) states defined by the 2×2 spin-matrix order parameter, $\hat{\Delta}(\mathbf{p}) = \Delta(\mathbf{p}) \hat{\mathbf{d}} \cdot (i\sigma\sigma_y)$, in which $\hat{\mathbf{d}}$ is the direction in spin space along which the Cooper pairs have zero spin projection. Equivalently, this state corresponds to equal amplitudes for the spin projections $S_u = +1$ and $S_u = -1$ with $\hat{\mathbf{u}} \perp \hat{\mathbf{d}}$. For the chiral A-phase of ${}^3\text{He}$, the direction $\hat{\mathbf{d}}$ can be controlled by a small magnetic field, \mathbf{B} , through the nuclear Zeeman energy that orients $\mathbf{d} \perp \mathbf{B}$. For chiral superconductors spin-orbit coupling and the crystalline field typically lock \mathbf{d} along a high-symmetry direction of the crystal.

We consider four classes of chiral ground states corresponding to the even-parity, spin-singlet, E_{1g} and E_{2g} , and odd-parity, spin-triplet, E_{1u} and E_{2u} representations of the

TABLE I. The representative basis functions, exhibiting chiral order, for the point groups D_{4h} and D_{6h} .

Point group	Irrep Γ	Basis function $\eta_{\Gamma}(\hat{\mathbf{p}})$	Chiral order ν	Parity
D_{4h}	E_g	$\hat{p}_z(\hat{p}_x + i\hat{p}_y) \propto \mathcal{Y}_2^1(\hat{\mathbf{p}})$	1	+
	E_u	$\hat{p}_x + i\hat{p}_y \propto \mathcal{Y}_1^1(\hat{\mathbf{p}})$	1	-
D_{6h}	E_{1g}	$\hat{p}_z(\hat{p}_x + i\hat{p}_y) \propto \mathcal{Y}_2^1(\hat{\mathbf{p}})$	1	+
	E_{2g}	$(\hat{p}_x + i\hat{p}_y)^2 \propto \mathcal{Y}_2^2(\hat{\mathbf{p}})$	2	+
	E_{1u}	$\hat{p}_x + i\hat{p}_y \propto \mathcal{Y}_1^1(\hat{\mathbf{p}})$	1	-
	E_{2u}	$\hat{p}_z(\hat{p}_x + i\hat{p}_y)^2 \propto \mathcal{Y}_3^2(\hat{\mathbf{p}})$	2	-

hexagonal point group, D_{6h} . These representations all allow for chiral ground states with principle winding numbers, $\nu = \pm 1$ ($\nu = \pm 2$) for the E_1 (E_2) representations.⁶⁰ Table I provides representative basis functions for these two-dimensional representations.

For even-parity, spin-singlet pairing the Nambu-matrix order parameter has the form, $\hat{\Delta}(\mathbf{p}) = (\Delta(\mathbf{p})\hat{\tau}_+ + \Delta^*(\mathbf{p})\hat{\tau}_-) \otimes (i\sigma_y)$, where $\hat{\tau}_{\pm} = (\hat{\tau}_1 \pm i\hat{\tau}_2)/2$ and $\{\hat{1}, \hat{\tau}_1, \hat{\tau}_2, \hat{\tau}_3\}$ are 2×2 matrices spanning particle-hole (Nambu) space. The spin-singlet correlations are represented by the Pauli matrix $i\sigma_y$, which is anti-symmetric under exchange. The orbital order parameter, $\Delta(\mathbf{p})$, is symmetric under exchange implying $\Delta(-\mathbf{p}) = +\Delta(\mathbf{p})$. The general form of the orbital order parameter is spanned by the two-dimensional space of $E_{1(2)g}$ basis functions. For E_{1g} the chiral basis $\{\mathcal{Y}_{\nu}(\mathbf{p})|\nu = \pm 1\}$ can be constructed from the 2D vector representation: $\mathcal{Y}_{\nu}(\mathbf{p}) = \mathcal{Y}_x(\mathbf{p}) + i\nu\mathcal{Y}_y(\mathbf{p}) = \sin(p_z a_z)(\hat{p}_x + i\nu\hat{p}_y) = \sin(p_z a_z)e^{i\nu\phi_{\mathbf{p}}}$, where the latter two forms correspond to E_{1g} basis functions defined on a cylindrical Fermi surface with $\phi_{\mathbf{p}}$ corresponding to the azimuthal angle of \mathbf{p} . Note that chiral E_{1g} pairing also breaks reflection symmetry in the plane normal to the chiral axis, and has a line of nodes in the energy gap for momenta in the plane $p_z = 0$. Thus, E_{1g} pairing is not realized in 2D, but is defined on a 3D Fermi surface.

For chiral E_{2g} pairing the basis functions can be defined as $\mathcal{Y}_{\nu}(\mathbf{p}) = \mathcal{Y}_{x^2-y^2}(\mathbf{p}) + i\text{sgn}(\nu)\mathcal{Y}_{xy}(\mathbf{p}) = (\hat{p}_x + i\text{sgn}(\nu)\hat{p}_y)^{|\nu|} = e^{i\nu\phi_{\mathbf{p}}}$, with $\nu = \pm 2$. The latter two forms correspond to E_{2g} pairing defined on a cylindrical Fermi surface. Note that the chiral ground state for E_{2g} also breaks reflection symmetry in one or more planes containing the chiral axis, $\hat{\ell} = \hat{\mathbf{z}}$, but, in contrast to E_{1g} , preserves

reflection symmetry in the plane normal to the chiral axis. Thus, a fully-gapped chiral ground state is possible in 2D, as well as a 3D Fermi surface that is open in the p_z direction. For a 3D Fermi surface that is closed in the p_z direction, the chiral E_{2g} ground state has topologically protected nodal points of $\Delta(\mathbf{p})$ at $\mathbf{p}_{\pm} = \pm p_f \hat{\mathbf{z}}$, and a corresponding spectrum of massless chiral Fermions in the bulk phase.³⁷

For odd-parity, ESP triplet states the Nambu-matrix order parameter takes the form, $\hat{\Delta}(\mathbf{p}) = (\Delta(\mathbf{p})\hat{\tau}_+ - \Delta^*(\mathbf{p})\hat{\tau}_-) \otimes (\sigma_x)$, where we have chosen the ESP state with $\hat{\mathbf{d}} = \hat{\mathbf{z}}$.⁶¹ The ESP triplet-correlations are represented by the symmetric Pauli matrix σ , and the odd-parity, order parameter, $\Delta(\mathbf{p})$, is necessarily anti-symmetric under exchange implying $\Delta(-\mathbf{p}) = -\Delta(\mathbf{p})$. For E_{1u} pairing the chiral basis $\{\mathcal{Y}_{\nu}(\mathbf{p})|\nu = \pm 1\}$ is constructed from the odd-parity 2D vector representation: $\mathcal{Y}_{\nu}(\mathbf{p}) = \mathcal{Y}_x(\mathbf{p}) + i\nu\mathcal{Y}_y(\mathbf{p}) = (\hat{p}_x + i\nu\hat{p}_y) = e^{i\nu\phi_{\mathbf{p}}}$, the latter two forms correspond to E_{1u} basis functions defined on a cylindrical Fermi surface with $\phi_{\mathbf{p}}$ corresponding to the azimuthal angle of \mathbf{p} . In contrast E_{1g} the E_{1u} chiral ground states are fully gapped in 2D, and in 3D for an open Fermi surface in the p_z direction. For chiral E_{2u} pairing the basis functions are constructed from those of E_{2g} by multiplying by odd-parity function of p_z . Thus, $\mathcal{Y}_{\nu}(\mathbf{p}) = \mathcal{Y}_{z(x^2-y^2)}(\mathbf{p}) + i\text{sgn}(\nu)\mathcal{Y}_{z(xy)}(\mathbf{p}) = \sin(p_z a_z)(\hat{p}_x + i\text{sgn}(\nu)\hat{p}_y)^2 = \sin(p_z a_z)e^{i\nu\phi_{\mathbf{p}}}$, with $\nu = \pm 2$. These chiral states correspond to the E_{2u} pairing model for the B-phase of UPT_3 .

A. 2D Chiral Superconductors

Here we consider the fully gapped E_{1u} and E_{2g} chiral ground states defined on a 2D cylindrical Fermi surface. These two cases illustrate nearly all of the key physical phenomena responsible for anomalous thermal and electrical transport mediated by non-magnetic impurity scattering in chiral superconductors. In Sec. VID we extend the theory to anomalous transport based on the 3D chiral states with line and point nodes.

At low temperatures, thermally excited quasiparticles and phonons are dilute, therefore quasiparticles interact predominantly with quenched defects. For randomly distributed impurities, the self-energy is given by $\hat{\Sigma}_{\text{imp}}(\hat{\mathbf{p}}; \varepsilon) = n_{\text{imp}}\hat{t}(\hat{\mathbf{p}}; \varepsilon)$, where n_{imp} is the impurity density and the single-impurity \hat{t} matrix in the superconducting state can be re-written in terms of the normal-state t-matrix which can be defined in terms of scattering phase shifts for normal-state quasiparticle-impurity scattering,

$$\hat{t}^{R,A}(\hat{\mathbf{p}}', \hat{\mathbf{p}}; \varepsilon) = \hat{t}_N^{R,A}(\hat{\mathbf{p}}', \hat{\mathbf{p}}) + N_f \left\langle \hat{t}_N^{R,A}(\hat{\mathbf{p}}', \hat{\mathbf{p}}'') \left[\hat{g}^{R,A}(\hat{\mathbf{p}}''; \varepsilon) - \hat{g}_N^{R,A} \right] \hat{t}^{R,A}(\hat{\mathbf{p}}'', \hat{\mathbf{p}}; \varepsilon) \right\rangle_{\hat{\mathbf{p}}''} \quad (26a)$$

$$\hat{t}^K(\hat{\mathbf{p}}', \hat{\mathbf{p}}; \varepsilon) = N_f \left\langle \hat{t}^R(\hat{\mathbf{p}}', \hat{\mathbf{p}}''; \varepsilon) \hat{g}^K(\hat{\mathbf{p}}''; \varepsilon) \hat{t}^A(\hat{\mathbf{p}}'', \hat{\mathbf{p}}; \varepsilon) \right\rangle_{\hat{\mathbf{p}}''}. \quad (26b)$$

Here N_f denotes the density of states per spin at the Fermi surface and $\langle \dots \rangle_{\hat{\mathbf{p}}}$ the Fermi-surface average — in isotropic systems, $\langle \dots \rangle_{\hat{\mathbf{p}}} = \int_0^{2\pi} d\phi_{\hat{\mathbf{p}}} / (2\pi) (\dots)$. The superscripts denote three types of quasiclassical propagators:

retarded (R), advanced (A) and Keldysh (K). In deriving Eq. (26), the bare electron-impurity interaction vertex is eliminated in favor of the normal-state propagator,

$\hat{g}_N = -\pi g_N \hat{\tau}_3$ with $g_N^R = (g_N^A)^* = i$, and \hat{t} matrix,

$$\hat{t}_N(\hat{\mathbf{p}}', \hat{\mathbf{p}}) = \frac{-1}{\pi N_f} \sum_{m=-\infty}^{+\infty} \frac{e^{im(\phi-\phi')}}{\cot \delta_m - g_N \hat{\tau}_3} \quad (27)$$

with δ_m the scattering phase shift in the m^{th} cylindrical harmonic⁶². Here and in the following, the Fermi directions $(\hat{\mathbf{p}}, \hat{\mathbf{p}}', \hat{\mathbf{p}}'', \dots)$ and their corresponding azimuth angles $(\phi, \phi', \phi'', \dots)$ are used interchangeably.

The mean field order parameter for fully gapped, unitary 2D chiral states can be expressed in the following form, $\hat{\Delta}_S(\mathbf{p}) = \hat{U}_S \hat{\Delta}(\mathbf{p}) \hat{U}_S^\dagger$, where \hat{U}_S is the unitary matrix for singlet ($S = 0$) or triplet ($S = 1$) pairing,

$$\hat{U}_0 = \begin{pmatrix} i\sigma_y & 0 \\ 0 & 1 \end{pmatrix}, \quad \hat{U}_1 = \begin{pmatrix} \hat{\mathbf{d}} \cdot i\sigma\sigma_y & 0 \\ 0 & 1 \end{pmatrix}, \quad (28)$$

and $\hat{\Delta}(\mathbf{p})$ reduces to

$$\hat{\Delta}(\mathbf{p}) = \Delta e^{iv\phi_{\mathbf{p}}} \hat{\tau}_3 (i\hat{\tau}_2) = \begin{pmatrix} 0 & \Delta e^{iv\phi_{\mathbf{p}}} \\ -\Delta e^{-iv\phi_{\mathbf{p}}} & 0 \end{pmatrix}, \quad (29)$$

for both $S = 0$ and $S = 1$. Thus, in the absence of external magnetic fields, magnetic impurities or spin-dependent perturbations, the spin structure of the order parameter can be transformed away by a unitary transformation, and as previously noted the quasiparticle excitation spectrum is doubly degenerate with respect to the quasiparticle spin.

This representation of the mean-field order parameter extends to the off-diagonal components of the impurity self energy. In Eq. 29 we chose Δ to be real. In this gauge the off-diagonal impurity self-energies reduce to

$$\hat{\Delta}_{\text{imp}}^{R,A}(\mathbf{p}; \varepsilon) = \Delta_{\text{imp}}^{R,A}(\varepsilon) e^{iv\phi_{\mathbf{p}}} \hat{\tau}_3 (i\hat{\tau}_2), \quad (30)$$

with the gauge condition, $\Delta_{\text{imp}}^{R,A}(\varepsilon) = \Delta_{\text{imp}}^{R,A}(-\varepsilon)^*$.⁶³ The Nambu-matrix impurity self energy can then be expressed in terms of three functions

$$\hat{\Sigma}_{\text{imp}}^{R,A}(\mathbf{p}; \varepsilon) = D_{\text{imp}}^{R,A}(\varepsilon) \hat{1} + \Sigma_{\text{imp}}^{R,A}(\varepsilon) \hat{\tau}_3 + \Delta_{\text{imp}}^{R,A}(\varepsilon) e^{iv\phi_{\mathbf{p}}} \hat{\tau}_3 (i\hat{\tau}_2). \quad (31)$$

The term proportional to the unit Nambu matrix, $D_{\text{imp}}^{R,A}(\varepsilon) \hat{1}$, drops out of Eq. 23 for the equilibrium propagators, $\hat{g}^{R,A}$, and thus plays no role in determining the equilibrium properties of the superconductor. However, the unit-matrix term does contribute to the linear response of the superconductor, e.g. the a.c. conductivity.⁶⁴

The diagonal term proportional to $\hat{\tau}_3$ can be combined with the excitation energy and expressed as

$$\tilde{\varepsilon}^{R,A}(\varepsilon) = \varepsilon - \Sigma_{\text{imp}}^{R,A}(\varepsilon), \quad (32)$$

and similarly the impurity renormalized off-diagonal self energy is given by

$$\tilde{\Delta}^{R,A}(\varepsilon) = \Delta + \Delta_{\text{imp}}^{R,A}(\varepsilon) \quad (33)$$

Thus, for any of the chiral, unitary states described by Eq. (30), the equilibrium propagators that satisfies the

transport equation and normalization condition, Eqs. (23) and (24), are given by

$$\hat{g}^{R,A}(\mathbf{p}; \varepsilon) = -\pi \frac{\tilde{\varepsilon}^{R,A} \hat{\tau}_3 - \tilde{\Delta}^{R,A} e^{iv\phi_{\mathbf{p}}} \hat{\tau}_3 (i\hat{\tau}_2)}{\sqrt{(\tilde{\Delta}^{R,A})^2 - (\tilde{\varepsilon}^{R,A})^2}} \quad (34)$$

$$\equiv -\pi [g^{R,A}(\varepsilon) \hat{\tau}_3 + f^{R,A}(\varepsilon) e^{iv\phi_{\mathbf{p}}} \hat{\tau}_3 (i\hat{\tau}_2)]. \quad (35)$$

Note that the functions $g^{R,A}$ and $f^{R,A}$ satisfy the symmetry relations: $g^A = (g^R)^*$ and $f^A = (f^R)^*$. In equilibrium, the Keldysh propagator is determined by the spectral functions for quasiparticles and Cooper pairs, and the thermal distribution of excitations,

$$\hat{g}^K(\mathbf{p}; \varepsilon) = (\hat{g}^R(\mathbf{p}; \varepsilon) - \hat{g}^A(\mathbf{p}; \varepsilon)) \tanh \frac{\varepsilon}{2T}. \quad (36)$$

Gap Equation: mean-field order parameter

The pairing interaction combined with the off-diagonal component of the Keldysh propagator determines the mean-field pairing self-energy for any of the unitary chiral states is given by the ‘‘gap equation’’,

$$\Delta(\mathbf{p}) = - \int d\mathbf{p}' \mu(\mathbf{p}, \mathbf{p}') \rlap{-}\int \frac{d\varepsilon'}{4\pi i} f^K(\mathbf{p}'; \varepsilon') \quad (37)$$

where the pairing interaction in any of the two-dimensional E-reps defined on a cylindrical Fermi surface has the form

$$\mu(\mathbf{p}, \mathbf{p}') = \mu_{|v|} \left(e^{-iv\phi_{\mathbf{p}}} e^{+iv\phi_{\mathbf{p}'}} + e^{+iv\phi_{\mathbf{p}}} e^{-iv\phi_{\mathbf{p}'}} \right) \quad (38)$$

$$= 2\mu_{|v|} \cos[v(\phi_{\mathbf{p}} - \phi_{\mathbf{p}'})]. \quad (39)$$

Thus, projecting out the amplitude of the chiral mean-field order parameter we obtain the gap equation,

$$\Delta = V \rlap{-}\int \frac{d\varepsilon}{4\pi i} (-\pi) [f^R(\varepsilon) - f^A(\varepsilon)] \tanh \frac{\varepsilon}{2T}. \quad (40)$$

$$(41)$$

In practice the vertex strength V is eliminated in favor of either the critical temperature or the gap value at zero temperature.

In equilibrium, the retarded and advanced propagators are given by

$$\hat{g}_{\text{eq}}(\hat{\mathbf{p}}; \varepsilon) = -\pi \frac{\tilde{\varepsilon}^{R,A}(\varepsilon) \hat{\tau}_3 - \tilde{\Delta}^{R,A}(\varepsilon) e^{i\hat{\tau}_3 v \phi} (i\hat{\tau}_2)}{C^{R,A}(\varepsilon)} \\ = -\pi \left[g(\varepsilon) \hat{\tau}_3 + f(\varepsilon) e^{i\hat{\tau}_3 v \phi} (i\hat{\tau}_2) \right] \quad (42)$$

where $g = \tilde{\varepsilon}/C$, $f = -\tilde{\Delta}/C$ and $C = [\tilde{\Delta}(\varepsilon)^2 - \tilde{\varepsilon}(\varepsilon)^2]^{1/2}$. Renormalized by interactions with defects, the equilibrium spectrum are given by $\tilde{\varepsilon} = \varepsilon - \Sigma_{\text{imp}}$ and $\tilde{\Delta} = \Delta_{\text{mf}} + \Delta_{\text{imp}}$, where Δ_{mf} is the mean-field excitation gap and Σ_{imp} and Δ_{imp} are defined in terms of the equilibrium self-energy⁶⁵

$$\hat{\Sigma}_{\text{imp}}(\hat{\mathbf{p}}; \varepsilon) = D(\varepsilon) \hat{1} + \Sigma_{\text{imp}}(\varepsilon) \hat{\tau}_3 + \Delta_{\text{imp}}(\varepsilon) e^{i\hat{\tau}_3 v \phi} (i\hat{\tau}_2). \quad (43)$$

The self-energy is obtained from the equilibrium \hat{t} matrix,

$$\begin{aligned}\hat{t}_{\text{eq}}(\hat{\mathbf{p}}', \hat{\mathbf{p}}; \varepsilon) &= \frac{-1}{\pi N_f} \begin{pmatrix} t(\hat{\mathbf{p}}', \hat{\mathbf{p}}; \varepsilon) & u(\hat{\mathbf{p}}', \hat{\mathbf{p}}; \varepsilon) \\ -\underline{u}(\hat{\mathbf{p}}', \hat{\mathbf{p}}; \varepsilon) & \underline{t}(\hat{\mathbf{p}}', \hat{\mathbf{p}}; \varepsilon) \end{pmatrix} \\ &= \frac{-1}{\pi N_f} \sum_m e^{im(\phi - \phi')} \begin{pmatrix} t_m(\varepsilon) & e^{iv\phi} u_{-m}(\varepsilon) \\ -e^{-iv\phi} \underline{u}_m(\varepsilon) & \underline{t}_{-m}(\varepsilon) \end{pmatrix}.\end{aligned}\quad (44)$$

Upon solving Eq. (26), we have

$$\begin{cases} t_m(\varepsilon) \\ \underline{t}_m(\varepsilon) \end{cases} = \frac{\sin \delta_m [\cos \delta_{m+v} \pm g(\varepsilon) \sin \delta_{m+v}]}{\cos(\delta_m - \delta_{m+v}) \mp g(\varepsilon) \sin(\delta_m - \delta_{m+v})} \quad (45a)$$

$$\begin{cases} u_m(\varepsilon) \\ \underline{u}_m(\varepsilon) \end{cases} = \frac{f(\varepsilon) \sin \delta_m \sin \delta_{m-v}}{\cos(\delta_m - \delta_{m-v}) \mp g(\varepsilon) \sin(\delta_m - \delta_{m-v})}.\quad (45b)$$

The off-diagonal pieces, u_m and \underline{u}_m , describe branch conversion scattering in which a Fermionic pair is formed or broken. To conserve angular momentum, such scattering only occurs between pairs of cylindrical harmonics which are compatible with the angular momentum of a Cooper pair. Therefore isotropic impurity scattering, i.e., point-like impurities, does not result in branch conversion scattering in chiral superconductors since the incoming and outgoing scattering states are both in the s -wave channel. Finally both the propagators and self-energies must be consistent with the weak-coupling gap equation

$$\Delta_{\text{mf}} = -V_0 \int \frac{d\varepsilon}{2} \tanh \frac{\varepsilon}{2T} \text{Im} f^R(\varepsilon), \quad (46)$$

where V_0 is the amplitude of the mean-field pairing vertex, $V(\hat{\mathbf{p}}, \hat{\mathbf{p}}') = 2V_0 \cos[v(\phi - \phi')]$.

V. LINEAR RESPONSE THEORY

For weak deviations from equilibrium, the heat current is proportional to the temperature gradient

$$\delta \mathbf{j}^{(\varepsilon)} = -\overset{\leftrightarrow}{\kappa} \cdot \nabla T, \quad (47)$$

where $\overset{\leftrightarrow}{\kappa}$ is the thermal conductivity, which is a tensor constrained by the symmetry of the ground state, in this a chiral ground state. To obtain linear transport coefficients, we self-consistently determine the equilibrium quasiclassical propagators *and* their non-equilibrium corrections through the linear order in perturbations. The equilibrium propagators are inputs to the linear-response calculations. They encode information about the quasiparticle spectrum. Heat currents are computed from the linear-response Keldysh propagator which encapsulates non-equilibrium corrections to the spectrum and occupation function.

We now consider the responses due to a static and homogeneous thermal gradient. Non-equilibrium corrections to the propagators and self-energies shall be parametrized as follows

$$\begin{aligned}\delta \hat{g}(\hat{\mathbf{p}}; \varepsilon) &= -\pi \sum_n e^{in\phi} \begin{pmatrix} \delta g_n(\varepsilon) & e^{iv\phi} \delta f_n(\varepsilon) \\ -e^{-iv\phi} \delta \underline{f}_n(\varepsilon) & \delta \underline{g}_n(\varepsilon) \end{pmatrix} \\ \delta \hat{\Sigma}(\hat{\mathbf{p}}; \varepsilon) &= \sum_n e^{in\phi} \begin{pmatrix} \delta \varepsilon_n(\varepsilon) & e^{iv\phi} \delta \Delta_n(\varepsilon) \\ -e^{-iv\phi} \delta \underline{\Delta}_n(\varepsilon) & \delta \underline{\varepsilon}_n(\varepsilon) \end{pmatrix}.\end{aligned}\quad (48)$$

We introduce also the anomalous responses

$$\delta \hat{x}^a(\varepsilon) = \delta \hat{x}^K(\varepsilon) - \tanh(\varepsilon/2T) [\delta \hat{x}^R(\varepsilon) - \delta \hat{x}^A(\varepsilon)], \quad (49)$$

where \hat{x} stands for propagators ($\hat{x} \rightarrow \hat{g}$) or self-energies ($\hat{x} \rightarrow \hat{\Sigma}$). In the following, we shall be concerned mainly with the anomalous functions, not least because the spectral responses do not contribute to the thermal conductivity in the quasiclassical linear response theory⁶⁶. Owing to the axial symmetry of the spectrum, the responses in different cylindrical harmonics are decoupled and given by (see, e.g.,⁶⁶, for a general solution)

$$|\delta g_n^a(\varepsilon)\rangle = \mathbb{L}^a(\varepsilon) [|\psi_n^a(\varepsilon)\rangle + |\delta \Sigma_n^a(\varepsilon)\rangle], \quad (50)$$

where \mathbb{L} is the linear-response operator, $|\delta \psi_n\rangle$ the external perturbation, $|\delta g_n\rangle = (\delta g_n, \delta \underline{g}_n, \delta f_n, \delta \underline{f}_n)^T$ and $|\delta \Sigma_n\rangle = (\delta \varepsilon_n, \delta \underline{\varepsilon}_n, \delta \Delta_n, \delta \underline{\Delta}_n)^T$. The linear-response operator is given by

$$\begin{aligned}\mathbb{L}^a(\varepsilon) &= -\mathcal{C}^a \begin{pmatrix} 1 + |g|^2 & -|f|^2 & -g^R f^A & -f^R g^A \\ -|f|^2 & 1 + |g|^2 & f^R g^A & g^R f^A \\ g^R f^A & -f^R g^A & 1 - |g|^2 & -|f|^2 \\ f^R g^A & -g^R f^A & -|f|^2 & 1 - |g|^2 \end{pmatrix} \\ &\quad - \mathcal{D}^a \begin{pmatrix} g^R - g^A & . & f^A & -f^R \\ . & -g^R + g^A & -f^R & f^A \\ -f^A & f^R & g^R + g^A & . \\ f^R & -f^A & . & -g^R - g^A \end{pmatrix},\end{aligned}\quad (51)$$

where $|g|^2 = g^R g^A$, $|f|^2 = f^R f^A$ and

$$\{\mathcal{C}^a(\varepsilon), \mathcal{D}^a(\varepsilon)\} = \frac{1}{2} \frac{\{\text{Re} C^R(\varepsilon), i \text{Im} D^R(\varepsilon)\}}{[\text{Re} C^R(\varepsilon)]^2 - [\text{Im} D^R(\varepsilon)]^2}.\quad (52)$$

A temperature gradient along the x axis generates a perturbation of the form

$$|\psi_n^a(\varepsilon)\rangle = \delta_{|n|,1} \psi_1^a(\varepsilon) (1, 1, \cdot, \cdot)^T \quad (53)$$

with $\psi_1^a(\varepsilon) = (iv_f/2) \partial_x \tanh[\varepsilon/2T(x)]$. We see that the *r.h.s.* of Eq. (50) consists of two terms. Explicitly proportional to the external field, the ‘direct’ contribution is equivalent to the relaxation-time approximation in the standard kinetic theory and does not yield transverse heat currents. Indeed the anomalous Hall effect arises from the term proportional to self-energy responses.

A. Self-Energy - Vertex Corrections

The self-energy corrections, which are ‘vertex corrections’ in field-theoretic calculations, describe the dynamical screening of perturbations by long-wavelength collective excitations⁵⁴. Within our linear response theory, the vertex corrections due to interactions with impurities are calculated from the linearized \hat{t} matrix equation. In the anomalous channel, the impurity self-energy is given by

$$\delta \hat{\Sigma}^a(\hat{\mathbf{p}}; \varepsilon) = n_{\text{imp}} N_f \langle \hat{t}^R(\hat{\mathbf{p}}, \hat{\mathbf{p}}'; \varepsilon) \delta \hat{g}^a(\hat{\mathbf{p}}'; \varepsilon) \hat{t}^A(\hat{\mathbf{p}}', \hat{\mathbf{p}}; \varepsilon) \rangle_{\hat{\mathbf{p}}'}.\quad (54)$$

Since the spectrum exhibits axial symmetry, each cylindrical harmonic decouples, yielding

$$|\delta\Sigma_n^a(\varepsilon)\rangle = -\frac{n_{\text{imp}}}{\pi N_f} \mathbb{T}_n^a(\varepsilon) |\delta g_n^a(\varepsilon)\rangle. \quad (55)$$

The vertex-correction operator is defined by

$$\mathbb{T}_n^a(\varepsilon) = \langle\langle \mathbb{Y}_n(\hat{\mathbf{p}})^* \mathbb{T}^a(\hat{\mathbf{p}}, \hat{\mathbf{p}}'; \varepsilon) \mathbb{Y}_n(\hat{\mathbf{p}}') \rangle\rangle_{\hat{\mathbf{p}}, \hat{\mathbf{p}}'}, \quad (56)$$

where $\mathbb{Y}_n(\hat{\mathbf{p}}) = e^{in\phi} \text{Diag}(1, 1, e^{iv\phi}, e^{-iv\phi})$ and

$$\mathbb{T}^a(\hat{\mathbf{p}}, \hat{\mathbf{p}}'; \varepsilon) = \begin{pmatrix} \underline{t}^R \underline{t}^A & -\underline{u}^R \underline{u}^A & -\underline{t}^R \underline{u}^A & -\underline{u}^R \underline{t}^A \\ -\underline{u}^R \underline{u}^A & \underline{t}^R \underline{t}^A & -\underline{u}^R \underline{t}^A & -\underline{t}^R \underline{u}^A \\ \underline{t}^R \underline{u}^A & \underline{u}^R \underline{t}^A & \underline{t}^R \underline{t}^A & -\underline{u}^R \underline{u}^A \\ \underline{u}^R \underline{t}^A & \underline{t}^R \underline{u}^A & -\underline{u}^R \underline{u}^A & \underline{t}^R \underline{t}^A \end{pmatrix}. \quad (57)$$

In the above, the retarded [advanced] \hat{t} matrix elements are evaluated at $(\hat{\mathbf{p}}, \hat{\mathbf{p}}'; \varepsilon)$ [$(\hat{\mathbf{p}}', \hat{\mathbf{p}}; \varepsilon)$]. Note that in general the mean-field pairing self-energies also contributes to vertex corrections, however this is present only in the retarded and advanced channels. The anomalous channel is subject only to impurity-induced vertex corrections. For point-like impurities, vertex corrections, and thus the anomalous Hall effect, vanish in all but chiral p -wave states. To see this, we write down the vertex correction due to isotropic scattering [see, Eq. (54)], $\delta\hat{\Sigma}(\varepsilon) \propto \langle\delta\hat{g}(\hat{\mathbf{p}}; \varepsilon)\rangle_{\hat{\mathbf{p}}}$ – i.e., only the isotropic components of the propagator responses contribute to vertex corrections. Now consider a p -wave perturbation, $\psi(\hat{\mathbf{p}}) \propto e^{i\phi}$. The diagonal pieces of the equilibrium propagators are isotropic, thus their linear responses acquire p -wave momentum dependence from the perturbation. Such p -wave terms vanish under Fermi-surface average and, as a result, cannot induce vertex corrections. On the other hand, the off-diagonal pieces of the equilibrium propagators contain the phase factor $e^{\pm iv\phi}$, encoding the angular momentum of a Cooper pair. Their linear responses carry a phase factor $e^{i(\pm v+1)\phi}$, which contributes to vertex corrections only when $|v| = 1$, i.e., chiral p -wave pairing. This is not a universal result. For finite-size impurities, vertex corrections and Hall effects are not limited to chiral p -wave states.

VI. RESULTS

To quantify the effects of finite-size impurities, we consider hard-disc scattering for which the scattering phase shifts are given by⁶⁷, $\tan \delta_m = J_{|m|}(k_f R)/N_{|m|}(k_f R)$, where R is the hard-disc radius and, $J_m(z)$ and $N_m(z)$ are the Bessel functions of the first and second kind, respectively. First we examine the equilibrium properties.

A. Suppression of T_c and Pair-breaking

The critical temperature, T_c , in disordered unconventional superconductors obeys^{68,69}

$$\ln \frac{T_{c0}}{T_c} = \Psi \left(\frac{1}{2} + \frac{1}{2} \frac{\xi_0 \sigma_{\text{pb}} n_{\text{imp}}}{T_c/T_{c0}} \right) - \Psi \left(\frac{1}{2} \right), \quad (58)$$

where $\Psi(x)$ is the digamma function and T_{c0} and $\xi_0 = v_f/2\pi T_{c0}$ denote the critical temperature and coherence length in a clean system. The pair breaking effect due to

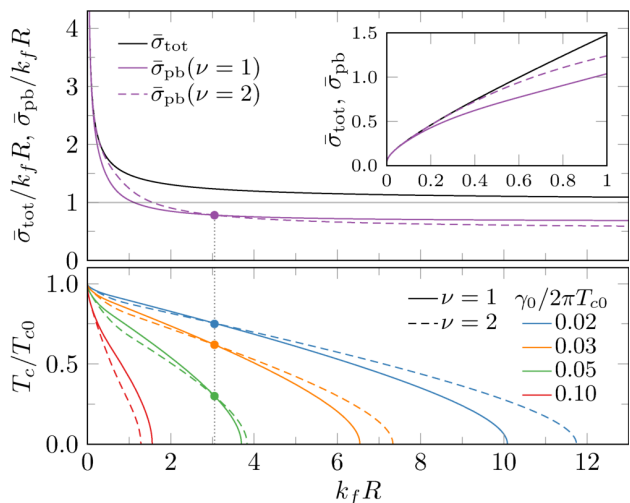


FIG. 1. Cross sections and critical temperature vs hard-disc radius for chiral states: $\nu = 1$ (solid) and $\nu = 2$ (dashed). For the hard-disc radius $k_f R \approx 3.05$, cross sections and critical temperature of the two states coincide (filled circles). *Top*: Total (black), transport (solid purple) and pair-breaking (purple) cross sections. *Bottom*: Critical temperature for various impurity densities (see legend).

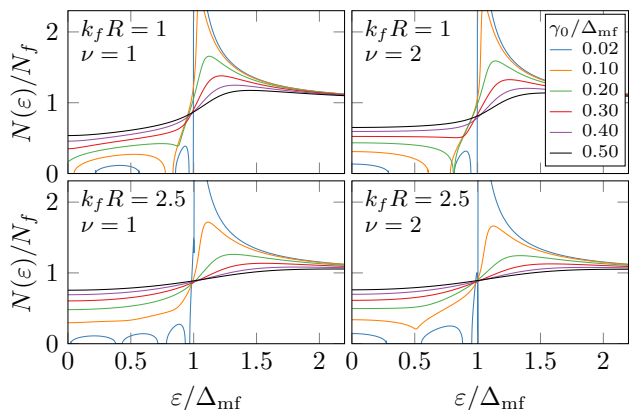


FIG. 2. Density of states for chiral order $\nu = 1$ (left) and $\nu = 2$ (right), various impurity densities normalized by $\xi_\Delta^2 = (\pi N_f \Delta_{\text{mf}})^{-1}$ (see legend), and impurity radii: $k_f R = 1$ (top) and 2.5 (bottom).

impurity scattering is characterized by the pair-breaking cross section

$$\sigma_{\text{pb}} = (2/k_f) \sum_m \sin^2(\delta_m - \delta_{m+\nu}) \quad (59)$$

for order parameters with winding number ν . This cross section vanishes for s -wave pairing ($\nu = 0$), yielding $T_c = T_{c0}$ as expected from Anderson's theorem.⁷⁰ Fig. 1 shows that σ_{pb} differs in general from the total cross section $\sigma_{\text{tot}} = (4/k_f) \sum_m \sin^2 \delta_m$ except in the small-impurity limit $k_f R \ll 1$. Furthermore we see that σ_{pb} and T_c depend on both the impurity radius and the chiral order. As a specific feature of the hard-disk scattering potential, σ_{pb} for $\nu = 2$ and $\nu = 1$ cross at $k_f R \approx 3.05$. At radii smaller (larger) than this value, pair breaking is stronger and T_c is lower for $\nu = 2$ ($\nu = 1$).

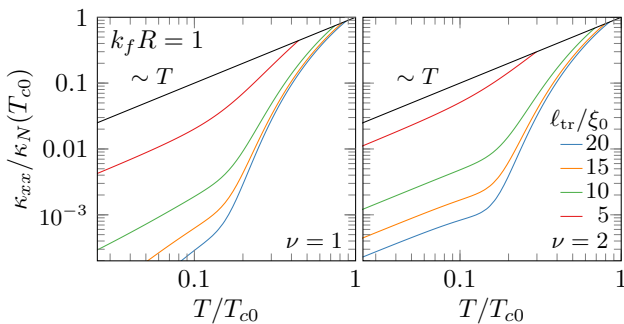


FIG. 3. Longitudinal thermal conductivity vs temperature for chiral order $\nu = 1$ (left) and $\nu = 2$ (right), impurity radius $k_f R = 1$, and various normal-state transport lengths (see legend). Normal-state thermal conductivity shown in black.

B. Density of States

The quasiparticle spectrum also depends sensitively on the chiral winding number. Consider the local density of states, $N(\varepsilon) = N_f \text{Im} g^R(\varepsilon)$. Figure 2 shows multiple sub-gap bound states which are broadened into bands with increasing impurity density. These states are formed via multiple Andreev scattering from the order parameter variations in momentum space, described by chiral order. As a result, the number of the bound states and the energies at which they occur depend not only on the structure of the impurity potential, e.g., the hard-disc radius, but also on the chiral winding number. This has important implications for transport phenomena, not least because transport in the limit $T \lesssim \Delta_{\text{mf}}$ is dominated by the lowest energy sub-gap states, without which currents are exponentially suppressed.

C. Thermal Conductivity & Anomalous Hall Effect

We now turn to thermal transport. In normal metals, the thermal conductivity, $\kappa_N = (\pi^2/3)N_f v_f L_N T$, is characterized by the transport mean free path $L_N = 1/(\sigma_{\text{tr}} n_{\text{imp}})$, defined in terms of the transport cross section $\sigma_{\text{tr}} = (2/k_f) \sum_m \sin^2(\delta_m - \delta_{m+1})^{71}$. In the superconducting state, the thermal conductivity reads

$$\kappa_{\{\text{xx}\}}(T) = N_f v_f \int d\varepsilon \left(\frac{\varepsilon}{2T} \text{sech} \frac{\varepsilon}{2T} \right)^2 L_{\{\text{xy}\}}(\varepsilon), \quad (60)$$

where we define the thermal transport lengths such that

$$L_{\text{xx}}(\varepsilon) \equiv \text{Re} \frac{v_f \delta g_1^a(\varepsilon)}{-2\Psi_1^a(\varepsilon)} \quad \text{and} \quad L_{\text{xy}}(\varepsilon) \equiv \text{Im} \frac{v_f \delta g_1^a(\varepsilon)}{-2\Psi_1^a(\varepsilon)}. \quad (61)$$

Figure 3 shows the temperature dependence of longitudinal thermal conductivity. While the presence of impurities generally enhances thermal conductivity through formations of sub-gap states, the effects depend on chiral order. For impurities with $k_f R = 1$, an Andreev bound state at $\varepsilon \approx 0$ develops for chiral order $\nu = 2$ but not for $\nu = 1$ (see, Fig. 2). This mid-gap ‘metallic’ band results in low-temperature thermal conductivity which is linear in temperature, i.e., $\kappa_{\text{xx}}(T \rightarrow 0) \propto T$. We see that such a behavior is always present for $\nu = 2$ whereas for $\nu = 1$ it occurs only at higher impurity densities where the impurity

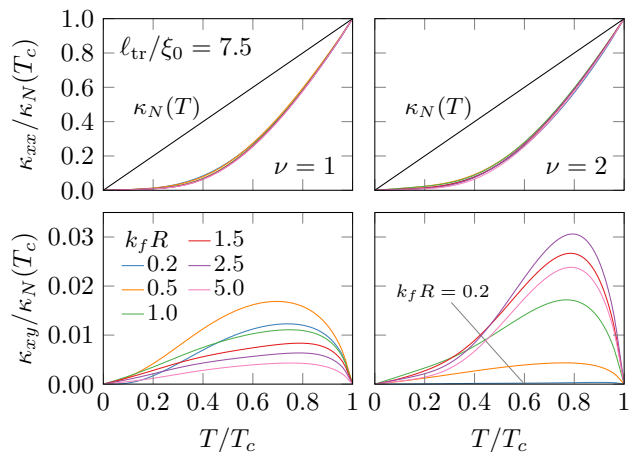


FIG. 4. Longitudinal (top) and transverse (bottom) thermal conductivity vs temperature for chiral order $\nu = 1$ (left) and $\nu = 2$ (right), normal-state transport length $L_N/\xi_0 = 7.5$, and various impurity radii (see legend). Normal-state thermal conductivity shown in black.

bands broaden to close the gap at $\varepsilon = 0$. Figure 4 illustrates perhaps the most pronounced effects of finite-size impurities on transport properties. Although longitudinal conductivity at temperature $T \gtrsim \Delta_{\text{mf}}$ is hardly affected by the impurity size or chiral order, the Hall conductivity depends strongly on both. When impurities are smaller than the inverse Fermi wavelength $k_f R \lesssim 1$ and impurity scattering is predominantly s -wave, the thermal Hall conductivity is severely suppressed for chiral states with $\nu = 2$ but remains finite for $\nu = 1$. This agrees with our previous argument that Hall currents vanish for point-like impurities, i.e., $k_f R \ll 1$, for all chiral orders but $|\nu| = 1$. On the other hand, for bigger impurities $k_f R > 1$, the Hall conductivity can be substantially larger in chiral states with $\nu = 2$, compared to $\nu = 1$. Furthermore, for a fixed normal-state transport mean free path, the Hall conductivity exhibits non monotonic dependence on the impurity size, reaching maximum at an intermediate radius. This suggests that the details of the impurity potential are of crucial importance for a quantitative understanding of the anomalous Hall effect in chiral superconductors.

Finally we compare low-temperature Hall transport due to edge states and impurities in the bulk. For chiral triplet p -wave pairing, the edge thermal Hall conductance is given by $K_{\text{xy}}^{\text{edge}} = \pi k_B^2 T / 6\hbar^{72-74}$ whereas the bulk conductance reads $K_{\text{xy}}^{\text{bulk}} = k_f L_{\text{xy}}^{\varepsilon=0} \pi k_B^2 T / 6\hbar$ [see, Eq. (60)]. While $K_{\text{xy}}^{\text{edge}}$ is fixed, $K_{\text{xy}}^{\text{bulk}}$ depends on the effective transport length $L_{\text{xy}}^{\varepsilon=0}$ which is finite only in a window of impurity density, see Fig. 5. Hall transport vanishes in the dirty limit due to the loss of chiral pairing, and bulk transport is absent in the clean limit due to the loss of impurity-induced states at $\varepsilon = 0$. When the spectrum is gapped at $\varepsilon = 0$, the edge contribution is expected to dominate as the bulk contribution vanishes. To compare the edge and bulk contributions when both are present, we must estimate material-specific parameters $k_f \xi_0$ and the impurity size $k_f R$. For example, taking $k_f \xi_0 = 100$ and $k_f R = 0.5$, we have $\max_{n_{\text{imp}}} K_{\text{xy}}^{\text{bulk}} \approx 35 K_{\text{xy}}^{\text{edge}}$. In general we find that when present, the bulk contribution tends to be dominant.

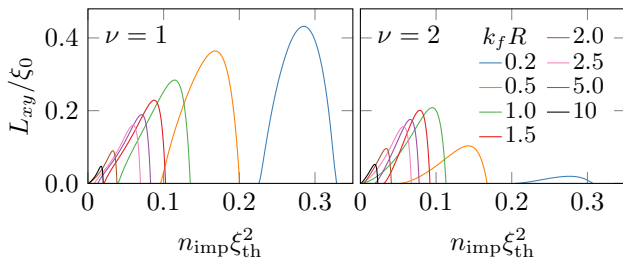


FIG. 5. Thermal Hall transport length at $\varepsilon = 0$ for chiral order $\nu = 1$ (left) and $\nu = 2$ (right), and varying impurity radii (see legend). Low-temperature transport requires quasiparticles states at $\varepsilon = 0$, formed only with adequate impurity density. But high impurity density destroys superconductivity and thus rules out any anomalous Hall effects.

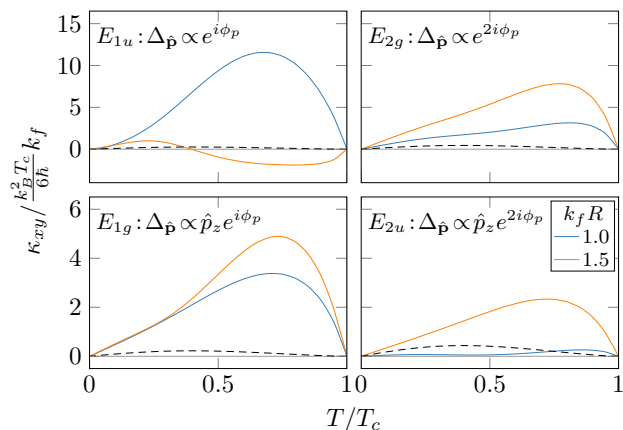


FIG. 6. The impurity-induced anomalous thermal Hall conductivity vs temperature for hard-sphere radii $k_f R = 1$ and 1.5 , and for the order parameter belonging to the irreducible representations, E_{1u} , E_{2g} , E_{1g} and E_{2u} (see labels), of the point group D_{6h} . The dashed curves depict the Berry phase contribution. Here we use the normal-state transport mean free path $L_N/\xi_0 = 7.5$ and a material parameter $k_f \xi_0 = 100$.

D. 3D Chiral Superconductors

The results for two dimensional chiral states is easily generalized to chiral states defined on closed 3D Fermi surfaces with line and point nodes. This includes the anomalous thermal Hall effects in three dimensional candidates for chiral superconductors, including Sr_2RuO_4 and the heavy-fermion compound UPt_3 .

Figure 6 depicts the anomalous thermal Hall conductivity for chiral superconductors belonging to the spin-triplet, odd-parity E_{1u} and E_{2u} representations and the spin-singlet, even-parity E_{1g} and E_{2g} representations of

the hexagonal D_{6h} point group, and E_u and E_g representations of D_{4h} . These representations cover nearly all of the proposed candidates for chiral superconductors, including Sr_2RuO_4 and the heavy-fermion compound UPt_3 . Crucially we see that the impurity-induced effects (solid lines) dominate the Berry curvature contribution^{75,76} (dashed lines) to the Hall conductivity in chiral pairing systems with finite-size impurities.

Finally we estimate the magnitude of the impurity-induced anomalous thermal Hall conductivity in UPt_3 . Taking $k_f = 1 \text{ \AA}^{-1}$, $\xi_0 = 100 \text{ \AA}$ and $T_c = 0.5 \text{ K}$ ⁷⁷, we obtain $\kappa_{xy} > 3 \times 10^{-3} \text{ WK}^{-1} \text{ m}^{-1}$ near T_c for the f -wave E_{2u} state with a hard-sphere impurity radius $k_f R = 1.5$ (see, Fig. 6). This value is well within the sensitivity of the current experimental techniques, which have measured $\kappa_{xy} < 10^{-3} \text{ WK}^{-1} \text{ m}^{-1}$ at $T < 1 \text{ K}$ ⁷⁸.

VII. CONCLUSIONS

We investigated the effects of finite-size impurities on chiral superconductors in two dimensions. In particular, a finite thermal Hall conductivity is obtained for superconductors with chiral winding $\nu = 1$ (p -wave) and $\nu = 2$ (d -wave). This contrasts with results obtained for point-like impurities in which transverse heat currents vanish in all but chiral p -wave states. We show further that the impurity-induced sub-gap states, formed via multiple Andreev scattering, depend strongly on the topology of chiral order as well as the structure of the impurity potential. Our estimate suggests that the thermal Hall currents induced by bulk impurities can be orders of magnitude larger than that due to edge states. As the bulk and edge Hall effects both originate from broken time-reversal and mirror symmetries, they are equally good indicators of chiral superconductivity. Indeed the bulk effect might be more experimentally accessible; not only can it produce stronger signals, but it is also less sensitive to the quality of the surfaces of a sample. In summary, our work provides quantitative formulae for interpreting heat transport experiments seeking to identify broken time-reversal symmetry and the topology of chiral superconductors.

VIII. ACKNOWLEDGEMENTS

The research of VN was supported through the Center for Applied Physics and Superconducting Technologies. The research of JAS was supported by the National Science Foundation (Grant DMR-1508730). We thank Pallab Goswami for discussions that informed this work.

* wave@northwestern.edu

† sauls@northwestern.edu

¹ A. P. Mackenzie and Y. Maeno, *The superconductivity of Sr_2RuO_4 and the physics of spin-triplet pairing*, Rev. Mod. Phys. **75**, 657 (2003).

² Y. Maeno, S. Kittaka, T. Nomura, S. Yonezawa, and K. Ishida, *Evaluation of Spin-Triplet Superconductivity in Sr_2RuO_4* , J. Phys. Soc. Japan **81**, 011009 (2012).

³ J. D. Strand, D. J. Van Harlingen, J. B. Kycia, and W. P. Halperin, *Evidence for Complex Superconducting Order Parameter Symmetry in the Low-Temperature Phase of UPt_3 from Josephson Interferometry*, Phys. Rev. Lett. **103**, 197002 (2009).

⁴ H. Ikegami, Y. Tsutsumi, and K. Kono, *Chiral Symmetry in Superfluid $^3\text{He-A}$* , Science **341**, 59 (2013).

⁵ O. Shevtsov and J. A. Sauls, *Electron Bubbles and Weyl Fermions in Chiral Superfluid $^3\text{He-A}$* , Phys. Rev. B **94**,

- 064511 (2016).
- ⁶ R. Nandkishore, L. S. Levitov, and A. V. Chubukov, *Chiral superconductivity from repulsive interactions in doped graphene*, Nature Physics **8**, 158 (2012).
 - ⁷ A. M. Black-Schaffer and K. Le Hur, *Topological superconductivity in two dimensions with mixed chirality*, Phys. Rev. B **92**, 140503 (2015).
 - ⁸ N. F. Q. Yuan, K. F. Mak, and K. T. Law, *Possible Topological Superconducting Phases of MoS_2* , Phys. Rev. Lett. **113**, 097001 (2014).
 - ⁹ P. K. Biswas, H. Luetkens, T. Neupert, T. Stürzer, C. Baines, G. Pascua, A. P. Schnyder, M. H. Fischer, J. Goryo, M. R. Lees, H. Maeter, F. Brückner, H.-H. Klauss, M. Nicklas, P. J. Baker, A. D. Hillier, M. Sigrist, A. Amato, and D. Johrendt, *Evidence for superconductivity with broken time-reversal symmetry in locally noncentrosymmetric $SrPtAs$* , Phys. Rev. B **87**, 180503 (2013).
 - ¹⁰ M. H. Fischer, T. Neupert, C. Platt, A. P. Schnyder, W. Hanke, J. Goryo, R. Thomale, and M. Sigrist, *Chiral d -wave superconductivity in $SrPtAs$* , Phys. Rev. B **89**, 020509 (2014).
 - ¹¹ T. M. Rice and M. Sigrist, *Sr_2RuO_4 : an electronic analogue of 3He ?* J. Phys. Cond. Mat. **7**, L643 (1995).
 - ¹² C. Kallin, *Chiral p -wave order in Sr_2RuO_4* , Reports on Progress in Physics **75**, 042501 (2012).
 - ¹³ G. Luke, Y. Fudamoto, K. Kojima, M. Larkin, J. Merriin, B. Nachumi, Y. Uemura, Y. Maeno, Z. Mao, Y. Mori, H. Nakamura, and M. Sigrist, *Time-reversal symmetry breaking superconductivity in Sr_2RuO_4* , Nature **394**, 558 (1998).
 - ¹⁴ J. Xia, Y. Maeno, P. Beyersdorf, M. Fejer, and A. Kapitulnik, *High Resolution Polar Kerr Effect Measurements of Sr_2RuO_4 : Evidence for Broken Time-Reversal Symmetry in the Superconducting State*, Phys. Rev. Lett. **97**, 167002 (2006).
 - ¹⁵ M. Matsumoto and M. Sigrist, *Quasiparticle States near the Surface and the Domain Wall in a $p_x + ip_y$ Wave Superconductor*, J. Phys. Soc. Japan **68**, 994 (1999).
 - ¹⁶ J. R. Kirtley, C. Kallin, C. W. Hicks, E.-A. Kim, Y. Liu, K. A. Moler, Y. Maeno, and K. D. Nelson, *Upper limit on spontaneous supercurrents in Sr_2RuO_4* , Phys. Rev. B **76**, 014526 (2007).
 - ¹⁷ C. W. Hicks, J. R. Kirtley, T. M. Lippman, N. C. Koshnick, M. E. Huber, Y. Maeno, W. M. Yuhasz, M. B. Maple, and K. A. Moler, *Limits on superconductivity-related magnetization in Sr_2RuO_4 and $PrOs_4Sb_{12}$ from scanning SQUID microscopy*, Phys. Rev. B **81**, 214501 (2010).
 - ¹⁸ P. J. Curran, S. J. Bending, W. M. Desoky, A. S. Gibbs, S. L. Lee, and A. P. Mackenzie, *Search for spontaneous edge currents and vortex imaging in Sr_2RuO_4 mesostructures*, Phys. Rev. B **89**, 144504 (2014).
 - ¹⁹ C. W. Hicks, D. O. Brodsky, E. A. Yelland, A. S. Gibbs, J. A. N. Bruin, M. E. Barber, S. D. Edkins, K. Nishimura, S. Yonezawa, Y. Maeno, and A. P. Mackenzie, *Strong Increase of T_c of Sr_2RuO_4 Under Both Tensile and Compressive Strain*, Science **344**, 283 (2014).
 - ²⁰ E. Hassinger, P. Bourgeois-Hope, H. Taniguchi, S. René de Cotret, G. Grissonnache, M. S. Anwar, Y. Maeno, N. Doiron-Leyraud, and L. Taillefer, *Vertical Line Nodes in the Superconducting Gap Structure of Sr_2RuO_4* , Phys. Rev. X **7**, 011032 (2017).
 - ²¹ M. J. Graf and A. V. Balatsky, *Identifying the pairing symmetry in the Sr_2RuO_4 superconductor*, Phys. Rev. B **62**, 9697 (2000).
 - ²² G. M. Luke, A. Keren, L. P. Le, W. D. Wu, Y. J. Uemura, D. A. Bonn, L. Taillefer, and J. D. Garrett, *Muon Spin Relaxation in UPt_3* , Phys. Rev. Lett. **71**, 1466 (1993).
 - ²³ D. Hess, T. A. Tokuyasu, and J. A. Sauls, *Broken Symmetry in an Unconventional Superconductor: A Model for the Double Transition in UPt_3* , J. Phys. Cond. Mat. **1**, 8135 (1989).
 - ²⁴ E. R. Schemm, W. J. Gannon, C. M. Wishne, W. P. Halperin, and A. Kapitulnik, *Observation of Broken Time-reversal Symmetry in the Heavy-Fermion Superconductor UPt_3* , Science **345**, 190 (2014).
 - ²⁵ K. Machida and M. Ozaki, *Splitting of Superconducting Transitions in UPt_3* , J. Phys. Soc. Jpn **58**, 2244 (1989).
 - ²⁶ A. Huxley, P. Rodiere, D. M. Paul, N. van Dijk, R. Cubitt, and J. Flouquet, *Re-alignment of the flux-line lattice by a change in the symmetry of superconductivity in UPt_3* , Nature **406**, 160 (2000).
 - ²⁷ J. D. Strand, D. J. Bahr, D. J. Van Harlingen, J. P. Davis, W. J. Gannon, and W. P. Halperin, *The Transition Between Real and Complex Superconducting Order Parameter Phases in UPt_3* , Science **328**, 1368 (2010).
 - ²⁸ J. A. Sauls, *The order parameter for the superconducting phases of UPt_3* , Adv. Phys. **43**, 113 (1994).
 - ²⁹ R. Joynt and L. Taillefer, *The superconducting phases of UPt_3* , Rev. Mod. Phys. **74**, 235 (2002).
 - ³⁰ More complex chiral order parameters with large winding numbers are allowed by the point group symmetry, c.f. Ref. 79; $v = \pm 1, \pm 2$ are the lowest order harmonics consistent with the E_1 and E_2 representations, respectively.
 - ³¹ C. Choi and J. Sauls, *Identification of Odd-Parity Superconductivity in UPt_3 Based on Paramagnetic Limiting of the Upper Critical Field*, Phys. Rev. Lett. **66**, 484 (1991).
 - ³² C. Choi and J. Sauls, *Anisotropy of the Upper Critical Field in Heavy Fermion Superconductors*, Phys. Rev. B **48**, 13684 (1993).
 - ³³ M. J. Graf, S.-K. Yip, and J. A. Sauls, *Thermal Conductivity of UPt_3 at Low Temperatures*, J. Low Temp. Phys. **102**, 367 (1996), (E) **106**, 727 (1997).
 - ³⁴ M. J. Graf, S.-K. Yip, and J. A. Sauls, *Thermal Conductivity of the Accidental Degeneracy and Enlarged Symmetry Group Models for Superconducting UPt_3* , J. Low Temp. Phys. **114**, 257 (1999).
 - ³⁵ M. J. Graf, S.-K. Yip, and J. A. Sauls, *Identification of the orbital pairing symmetry in UPt_3* , Phys. Rev. B **62**, 14393 (2000).
 - ³⁶ W. J. Gannon, W. P. Halperin, C. Rastovski, K. J. Schlessinger, J. Hlevyack, M. R. Eskildsen, A. B. Vorontsov, J. Gavilano, U. Gasser, and G. Nagy, *Nodal gap structure and order parameter symmetry of the unconventional superconductor UPt_3* , New. J. Phys. **17**, 023041 (2015).
 - ³⁷ P. Goswami and A. H. Nevidomskyy, *Topological Weyl superconductor to diffusive thermal Hall metal crossover in the B phase of UPt_3* , Phys. Rev. B **92**, 214504 (2015).
 - ³⁸ Y. Tsutsumi and K. Machida, *Edge mass current and the role of Majorana fermions in A-phase superfluid 3He* , Phys. Rev. B **85**, 100506 (2012).
 - ³⁹ N. Read and D. Green, *Paired states of Fermions in two dimensions with breaking of parity and time-reversal symmetries and the fractional quantum Hall effect*, Phys. Rev. B **61**, 10267 (2000).
 - ⁴⁰ M. Stone and R. Roy, *Edge modes, edge currents, and gauge invariance in $p_x + ip_y$ superfluids and superconductors*, Phys. Rev. B **69**, 184511 (2004).
 - ⁴¹ J. A. Sauls, *Surface states, Edge Currents, and the Angular Momentum of Chiral p -wave Superfluids*, Phys. Rev. B **84**, 214509 (2011).
 - ⁴² H. Sumiyoshi and S. Fujimoto, *Quantum Thermal Hall Effect in a Time-Reversal-Symmetry-Broken Topological Superconductor in Two Dimensions: Approach from Bulk Calculations*, J. Phys. Soc. Japan **82**, 023602 (2013).
 - ⁴³ T. Qin, Q. Niu, and J. Shi, *Energy Magnetization and the Thermal Hall Effect*, Phys. Rev. Lett. **107**, 236601 (2011).
 - ⁴⁴ Time-reversal and mirror symmetries need not be broken simultaneously. For example, a three-band superconductor may break time-reversal symmetry when the order parameters for each band have different phases, resulting in Josephson currents between the Fermi sheets. The mirror symmetry is however preserved and Hall effects are therefore not expected in

- this system.
- ⁴⁵ B. Arfi, H. Bahlouli, C. J. Pethick, and D. Pines, *Unusual transport effects in anisotropic superconductors*, Phys. Rev. Lett. **60**, 2206 (1988).
- ⁴⁶ S. Li, A. V. Andreev, and B. Z. Spivak, *Anomalous transport phenomena in $p_x + ip_y$ superconductors*, Phys. Rev. B **92**, 100506 (2015).
- ⁴⁷ S. Yip, *Low temperature thermal hall conductivity of a nodal chiral superconductor*, Supercond. Sci. Technol. **29**, 085006 (2016).
- ⁴⁸ L. V. Keldysh, *Diagram Technique for Nonequilibrium Processes*, Zh. Eksp. Teor. Fiz. **47**, 1515 (1965), english: Sov. Phys. JETP, **20**, 1018 (1965).
- ⁴⁹ G. Eilenberger, *Transformation of Gorkov's Equation for Type II Superconductors into Transport-Like Equations*, Zeit. f. Physik **214**, 195 (1968).
- ⁵⁰ A. I. Larkin and Y. N. Ovchinnikov, *Quasiclassical Method in the Theory of Superconductivity*, Sov. Phys. JETP **28**, 1200 (1969).
- ⁵¹ A. Larkin and Y. Ovchinnikov, *Nonlinear conductivity of superconductors in the mixed state*, Sov. Phys. JETP **41**, 960 (1976).
- ⁵² J. W. Serene and D. Rainer, *The Quasiclassical Approach to ^3He* , Phys. Rep. **101**, 221 (1983).
- ⁵³ A. I. Larkin and Y. N. Ovchinnikov, in *Modern Problems in Condensed Matter Physics*, edited by D. Langenberg and A. Larkin (Elsevier Science Publishers, Amsterdam, 1986).
- ⁵⁴ D. Rainer and J. A. Sauls, *Strong-Coupling Theory of Superconductivity*, in *Superconductivity: From Basic Physics to New Developments* (World Scientific, Singapore, 1994) Chap. 2, pp. 45–78, arXiv:https://arxiv.org/abs/1809.05264.
- ⁵⁵ M. J. Graf, S.-K. Yip, J. A. Sauls, and D. Rainer, *Electronic Thermal Conductivity and the Wiedemann-Franz Law for Unconventional Superconductors*, Phys. Rev. B **53**, 15147 (1996).
- ⁵⁶ Include case with $A(\epsilon)$ only.
- ⁵⁷ D. Rainer, in *Progress in Low Temperature Physics*, Vol. 10 (Elsevier Science Publishers B.V., Amsterdam, 1986) pp. 371–424.
- ⁵⁸ The separation does not apply to superconducting materials without an inversion center, i.e. non-centro-symmetric superconductors.
- ⁵⁹ The A_1 phase of superfluid ^3He , which is stabilized by an externally applied magnetic field, is a non-unitary spin-triplet state.⁸⁰ The Uranium-based ferromagnetic superconductors are also believed to be non-unitary, spin-polarized, triplet superconductors.
- ⁶⁰ For a cylindrical Fermi surface with *continuous* 2D rotational symmetry, $D_{\infty h}$, chiral ground states with any integer winding number $\nu \in \mathcal{Z}$ are possible. For the discrete point group D_{6h} higher winding numbers with $\nu = \pm 1 + \text{mod}(6)$ (E_1) or $\nu = \pm 2 + \text{mod}(6)$ (E_2) are possible for pairing basis functions exhibiting strong hexagonal anisotropy, but in general the chiral basis functions with higher winding numbers will mix with $\nu = \pm 1$ ($\nu = \pm 2$).
- ⁶¹ The results for the heat and charge transport in zero field do not depend on the choice for the direction of \mathbf{d} .
- ⁶² The summation over m is truncated as a defect with characteristic radius R leads to rapidly decaying phase shifts for $|m| \gtrsim k_f R$.
- ⁶³ For a cylindrical Fermi surface the directions $\{\hat{p}, \hat{p}', \hat{p}'', \dots\}$ and the corresponding azimuthal angles $\{\phi, \phi', \phi'', \dots\}$ are used interchangeably.
- ⁶⁴ M. J. Graf, M. Palumbo, D. Rainer, and J. A. Sauls, *Infrared Conductivity in Layered d-wave Superconductors*, Phys. Rev. B **52**, 10588 (1995).
- ⁶⁵ Despite being absent from spectral renormalization, $D^{R,A}(\epsilon)$ encodes particle-hole asymmetry, e.g., the difference in scattering lifetimes for particles and holes, which could have implications for transport properties⁸¹, especially in thermoelectric responses⁸².
- ⁶⁶ M. J. Graf, S.-K. Yip, J. A. Sauls, and D. Rainer, *Electronic thermal conductivity and the Wiedemann-Franz law for unconventional superconductors*, Phys. Rev. B **53**, 15147 (1996).
- ⁶⁷ I. R. Lapidus, *Scattering by twodimensional circular barrier, hard circle, and delta function ring potentials*, Am. J. Phys. **54**, 459 (1986).
- ⁶⁸ A. I. Larkin and Y. N. Ovchinnikov, *Vector Paring in Superconductors in Small Dimensions*, Sov. Phys. JETP **2**, 130 (1965).
- ⁶⁹ E. V. Thuneberg, S.-K. Yip, M. Fogelström, and J. A. Sauls, *Scattering Models for Superfluid ^3He in Aerogel*, Phys. Rev. Lett. **80**, 2861 (1998), [Original Version: condmat/9601148v2].
- ⁷⁰ P. Anderson, *Theory of Dirty Superconductors*, J. Phys. Chem. Sol. **11**, 26 (1959).
- ⁷¹ The transport and pair-breaking cross sections are generally different except for $|v| = 1$, see Eq. (59).
- ⁷² N. Read and D. Green, *Paired states of fermions in two dimensions with breaking of parity and time-reversal symmetries and the fractional quantum hall effect*, Phys. Rev. B **61**, 10267 (2000).
- ⁷³ T. Senthil, J. B. Marston, and M. P. A. Fisher, *Spin quantum hall effect in unconventional superconductors*, Phys. Rev. B **60**, 4245 (1999).
- ⁷⁴ H. Sumiyoshi and S. Fujimoto, *Quantum thermal hall effect in a time-reversal-symmetry-broken topological superconductor in two dimensions: Approach from bulk calculations*, J. Phys. Soc. Jpn. **82**, 023602 (2013).
- ⁷⁵ T. Qin, Q. Niu, and J. Shi, *Energy magnetization and the thermal hall effect*, Phys. Rev. Lett. **107**, 236601 (2011).
- ⁷⁶ P. Goswami and A. H. Nevidomskyy, *Topological weyl superconductor to diffusive thermal hall metal crossover in the B phase of UPt_3* , Phys. Rev. B **92**, 214504 (2015).
- ⁷⁷ R. Joynt and L. Taillefer, *The superconducting phases of UPt_3* , Rev. Mod. Phys. **74**, 235 (2002).
- ⁷⁸ M. Hirschberger, R. Chisnell, Y. S. Lee, and N. P. Ong, *Thermal hall effect of spin excitations in a kagome magnet*, Phys. Rev. Lett. **115**, 106603 (2015).
- ⁷⁹ T. Scaffidi and S. H. Simon, *Large Chern Number and Edge Currents in Sr_2RuO_4* , Phys. Rev. Lett. **115**, 087003 (2015).
- ⁸⁰ V. Ambegaokar and N. D. Mermin, *Thermal Anomalies of ^3He Pairing in a Magnetic Field*, Phys. Rev. Lett. **30**, 81 (1973).
- ⁸¹ B. Arfi, H. Bahlouli, and C. J. Pethick, *Transport properties of anisotropic superconductors: Influence of arbitrary electron-impurity phase shifts*, Phys. Rev. B **39**, 8959 (1989).
- ⁸² T. Löfwander and M. Fogelström, *Large thermoelectric effects in unconventional superconductors*, Phys. Rev. B **70**, 024515 (2004).